An Intelligent System for Energy-Efficient Lighting and Illuminance Control in Buildings

by

Sepehr Attarchi

B.Sc., Mazandaran University, 2005

Thesis Submitted in Partial Fulfillment of the
Requirements for the Degree of
Master of Applied Science

in the
Mechatronic Systems Engineering
Faculty of Applied Science

SIMON FRASER UNIVERSITY

Spring 2014

Approval

Name:	**Sepehr Attarchi**
Degree:	**Master of Applied Science (Mechatronic Systems Engineering)**
Title of Thesis:	***An Intelligent System for Energy-efficient Lighting and Illuminance Control in Buildings***
Examining Committee:	**Chair:** Siamak Arzanpour Assistant Professor of Mechatronic Systems Engineering

Mehrdad Moallem
Senior Supervisor
Professor of Mechatronic Systems Engineering

Ahmad Rad
Supervisor
Professor of Mechatronic Systems Engineering

Craig Scratchley
Internal Examiner
Senior Lecturer of Engineering Science

Date Defended/Approved: March 4, 2014

Partial Copyright Licence

Abstract

Visual comfort and energy saving are two main aspects of an intelligent lighting system. Although the modern lighting systems have been able to achieve major energy savings through different lighting control strategies, the users' visual preferences have been generally neglected in these systems. Human perception has always been an important factor affecting the overall performance of a lighting system. Not much of the studies carried out in this field have focused on delivering the desired illuminance to the users. Not to mention that frequent changes or noticeable jumps in the output light levels could also be very annoying for the users. The contribution of this thesis is twofold: First, a robust communication framework was developed which is a major pre-requisite for deployment of any lighting system. The developed framework is responsible for facilitating the communication between various types of hardware such as motion, and light sensors, as well as light actuators in the network. Secondly, daylight harvesting, motion detection, and light level tuning strategies were explored by utilizing the developed lighting system infrastructure. In particular, a lighting control algorithm was proposed for residential and commercial use, which when integrated with a building automation system, can satisfy the visual preferences of the users while reducing the overall amount of energy usage in the system. In open-plan environments, the proposed algorithm is capable of delivering the desired light levels for each occupant. The effectiveness of the developed lighting system and the proposed control algorithm were verified by a proof-of-concept testbed and pilot implementations.

Keywords: Control systems; Energy saving; Illuminance control; Intelligent lighting; Wireless sensor network

Acknowledgement

I would like to express my gratitude to anyone who helped me in this project. I would like to thank my supervisor, Dr. Mehrdad Moallem, for his advices, patience, and assistance during the entire project. His guidance and inspirations have provided an invaluable experience that will help me in the rest of my life. I am also grateful to Dr. Ahmad Rad and Dr. Craig Scratchley for taking the time to serve as my committee members. My special thanks to my colleagues, especially Yaser M. Roshan, Ali Shagerdmootaab, Rasoul Milasi, Younes Rashidi, Amir Maravandi, Masoud Nosrati, Farzad Hamidi, Soroush Sefidkar, Shahrzad Faghihi, Armin Alaghi and Samaneh Khakshour for their continued support and kind suggestions.

Last but not least, I would like to thank my family in Iran. My father, for being an unending source of encouragement and hope, and my mother and sister for their constant love and support and sacrifices.

Table of Contents

List of Tables

List of Figures

List of Acronyms

AES	Advanced Encryption Standard
BAS	Building Automation System
BLE	Bluetooth Low Energy
BPSK	Binary Phase Shift Keying
BRE	Bit Rate Error
CFL	Compact Fluorescent Light
CRC	Cyclic Redundancy Check
CSMA-CA	Carrier Sense Multiple Access with Collision Avoidance
EIA	U.S. Energy Information Administration
FDMA	Frequency-Division Multiple Access
FHSS	Frequency Hopping Spread Spectrum
GFSK	Gaussian Frequency Shift Keying
GUI	Graphical User Interface
HVAC	Heating, Ventilation and Air Conditioning
IEA	International Energy Agency
IP	Internet Protocol
ISM	Industrial, Scientific and Medical
LED	Light Emitting Diode
LQR	Linear Quadratic Regulator
MAC	Media Access Layer
MIMO	Multiple-Input, Multiple-output
OLS	Ordinary Least Square
OSI	Open System Interconnection

OECD	Organisation of Economic Co-operation and Development
PAN	Personal Area Network
PHY	Physical Layer
PSL	Phase Shift Keying
PWM	Pulse Width Modulation
QPSK	Quadrature Phase Shift Keying
SNR	Signal to Noise Ratio
TCP	Transmission Control Protocol
UART	Universal Asynchronous Receiver/Transmitter
WBAN	Wireless Body Area Network
WLAN	Wireless Local Area Network
WSN	Wireless Sensor Network

Chapter 1. Introduction

The growing usage of energy in the world has raised concerns about the energy supplies, depletion of energy resources, and its severe environmental impacts. According to the data gathered by the International Energy Agency (IEA), the world total energy usage has raised by 39% during the last two decades (Table 1.1) [1], [2]. This prospect could be even worse considering the fact that the energy usage by the nations with emerging economics (Southeast Asia, South America, Middle East, etc.) will exceed their counterparts in the developed countries by 2025 (Figure 1.1) [3].

The gathered data suggest correlations between the total energy consumption, population, and economic growth of the world. The main conclusion that can be drawn from these data is that energy consumption has been growing at a higher rate than the world's population over the last two decades. The data also suggests that worldwide attempts to reduce the amount of energy consumption through energy saving measures and green technologies may not have been good enough so far.

Table 1.1. Total Primary energy consumption and growth 1990-2008. Source: IEA/OECD.

	Population (Million)			Energy use (1000 Terawatt-hour)		
	1990	2008	Growth	1990	2008	Growth
USA	250	305	22%	22.3	26.6	20%
EU-27	473	499	5%	19.0	20.4	7%
Middle East	132	199	51%	2.6	6.9	170%
China	1141	1333	17%	10.1	24.8	146%
Latin America	355	462	30%	4.0	6.7	66%
Africa	634	984	55%	4.5	7.7	70%
India	850	1140	34%	3.8	7.2	91%
Others	1430	1766	23%	36.1	42.2	17%
The world	5265	6688	27%	102.3	142.3	39%

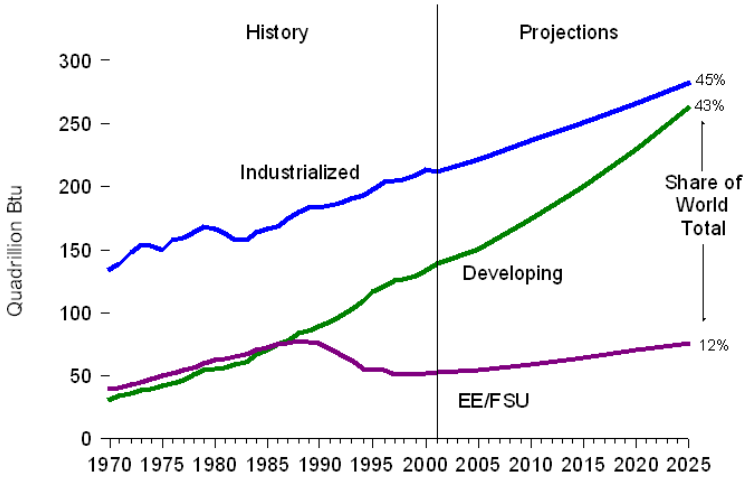

Figure 1.1. World marketed energy consumption by region. Source: EIA, international energy outlook 2004.

The energy usage is usually split into four major end-use sectors: industry, transport, residential, and commercial. Based on reports by the U.S. energy information administration, nearly 40% of the total U.S. energy consumption in 2011 was consumed in residential and commercial buildings (Figure 1.2) [3]. Recent growth in the world's population, improvement in building services and their comfort level, along with longer times spent inside buildings, have increased the total energy consumption in the residential and commercial buildings to the levels comparable with the transportation facilities and industrial plants. Thus it might be soon very crucial to perform a comprehensive study on building energy consumption, its utilization breakdown, and various methods to reduce the amount of energy consumption in buildings.

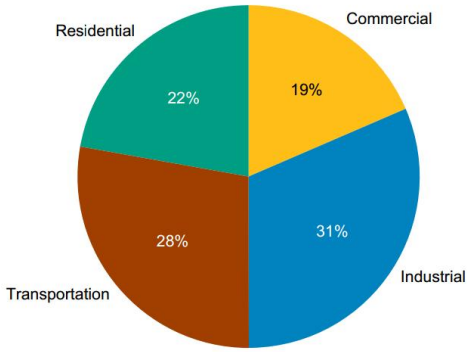

Figure 1.2. End-use sector share of total energy consumption in 2011. Source: EIA.

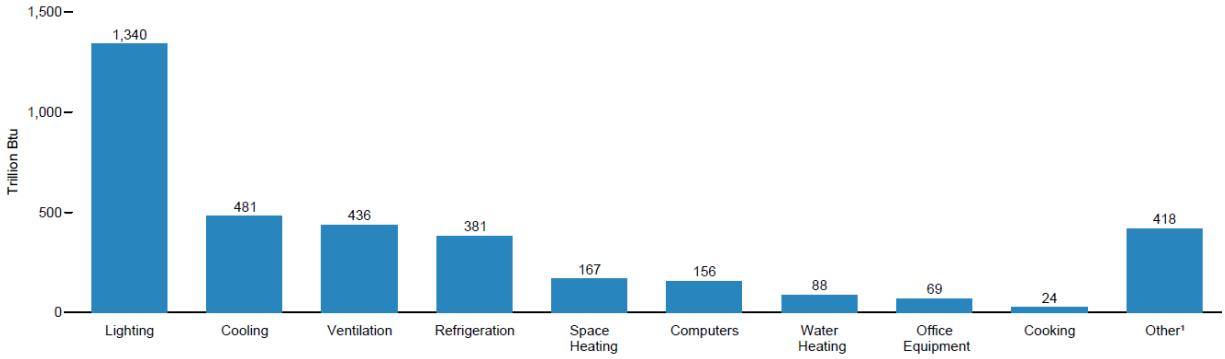

Figure 1.3. Commercial building electricity consumption by end-use in 2003. Source: EIA.

Figure 1.3 demonstrates the electricity consumption breakdown in commercial buildings by end-uses. According to these numbers (published in September 2012 by EIA), about 38% of the total electricity consumption in the buildings is used for the lighting purposes. Figure 1.4 also indicates the electricity consumption in commercial buildings sorted by principle building activities. Obtained data by EIA confirms that the lighting is undoubtedly a main contributor to the total electricity power consumption in commercial and residential buildings. As a matter of fact, over 70% the total energy is consumed by lighting and HVAC systems in commercial and residential buildings. These realities, along with ongoing rise in the cost of energy worldwide, have motivated the researchers and developers to seek new techniques in order to reduce the amount of energy consumption in the buildings. Reducing the consumption of non-renewable energy would also have significant impact on the environment worldwide.

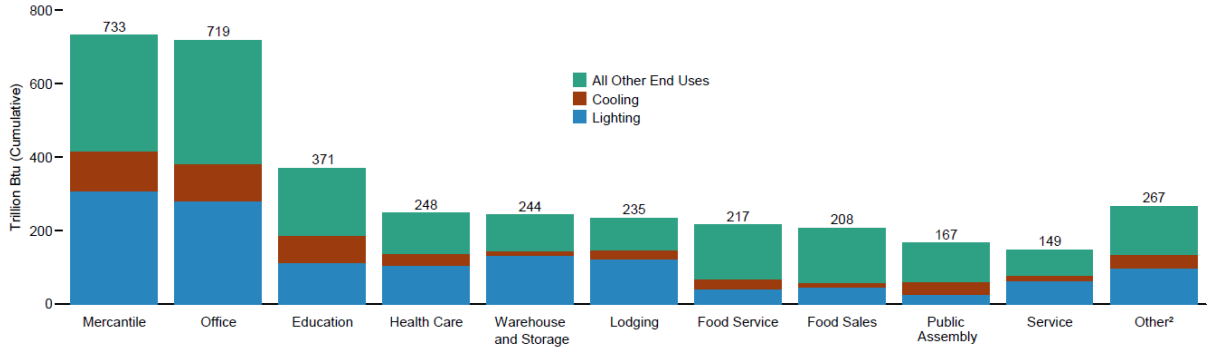

Figure 1.4. Commercial building electricity consumption by principle building activity, 2003. Source: EIA.

Nowadays reducing the amount of energy usage in buildings can be achieved by using modern smart automation systems in commercial and residential sectors. Deployment of an intelligent lighting system is an efficient way to reduce the amount of energy usage in different environments (e.g., home, office) while satisfying the photometric features and users' preferences. During the last decades, various types of electrical appliances, airplanes, automobiles, and a variety of other systems have become more intelligent. This intelligence is mainly due to the improvement in automated control of system's own operation to suit the user preferences and environmental conditions. Although systems are becoming more intelligent, the intelligence has not been fully applied to the lighting systems yet. Recent improvements in this area have been mostly focused on controlling the output light of different fixture individually. Also many techniques have been studied for preserving energy consumption using the daylight harvesting concept. For instance, predefined time switching patterns and ambient light control have been developed to include efficient use of daylight and eventually reducing the amount of energy consumption.

Still many problems remain unsolved in the area of lighting control. With the current trend in intelligent lighting systems, it is impossible to provide a desired illuminance to an arbitrary location in the installation area. In fact, each individual may feel more comfortable with different light levels when performing certain tasks or activities. For example, low light levels are more suitable for watching movies at home, while brighter lights may be more favourable for other activities like studying, reading etc.

Other shortcomings of current intelligent lighting systems could be the inability to allow the fixtures to compensate for the others in the case of a fixture failure. Also, with any changes in the design of the installation area, current systems are not capable of adapting to new designs and provide flexible response to new preferences.

The available lighting systems commonly operate in conjunction with traditional luminaires, including fluorescent and incandescent lights. But difficulties in synchronously adjusting the intensity and color spectrum of traditional lights make these types of luminaires unsuitable to be used in intelligent lighting systems. On the other hand, Light Emitting Diode (LED) luminaires are capable of preserving light color and lumen efficacy in a wider range. They are also easily dimmable, which makes them more suitable for adopting in intelligent control systems. This could be the main reason for the rising interest

in adoption of LED luminaires in daily lighting and intelligent lighting systems in the buildings.

The most basic types of intelligent lighting systems usually use motion, occupancy, and ambient light sensors. These systems prevent energy waste by turning on the lights when someone enters or stays in a room and automatically turn them off when there is no activity in the room for a pre-defined period of time. Ambient lights sensor also help in reducing the amount of energy consumption by forcing the luminaires to go off when there is enough light during the daylight hours. They are also useful in adjusting the amount of light inside a building by measuring the ambient light levels. A brief introduction to the intelligent lighting system and its existing variation is presented in the next section.

1.1. Overview of Intelligent Lighting Systems

The term “intelligent lighting system” refers to a lighting system in which each luminaire can communicate with its counterparts through a wireless or wired network and the user needs are met by cooperation of the connected luminaires in the network [4]. More precisely, an intelligent lighting system is a system with multiple luminaires which has

1. Occupancy and/or motion sensors that can detect the presence of any individual,
2. Ambient light sensors capable of measuring the light level locally,
3. The capability to change power to individual lights and their output lumens,
4. The communication infrastructure to exchange information across luminaires and the local control unit.

The ultimate objective of such a system would be providing energy saving while satisfying the visual preferences of the users. In such a system, the user specifies a desired illuminance on a specific location and the system will automatically adjust the lightings to provide the target illuminance.

Based on the infrastructure of installation site and also the user needs, two possible lighting control schemes can be adopted by the lighting systems:

(a) Autonomous distributed control:

In this type of control system, there is no central unit controlling the entire system. Each luminaire controls its output light autonomously and based on the feedback received by its own ambient light sensor. These systems usually have high robustness against malfunctioning since failure in a particular fixture doesn't affect the others in the entire system. It is also easy to add or remove light fixtures and sensors without affecting the rest of luminaires, making this type of systems more reliable for large scale installations.

(b) Centralized control:

In this type of control system, there is at least one central unit which is responsible for making decisions for the entire system based on sensory feedback. In other words, there is no autonomous decision making by the individual luminaires and the output values of the luminaires are decided by a central controller which are sent out to all the luminaires simultaneously. Compared with autonomous distributed systems, this type of control is less robust against the malfunctioning of fixtures, since failure in a particular fixture will affect the output of entire luminaires in the system. Commissioning of this type of systems are more difficult when settings like node ID, node location, and layout information for each luminaire or light sensor are required during the installation. However, the centralized control systems are inherently more intelligent, enabling them to use various control algorithms on the central control unit to satisfy the user needs in addition to reducing energy consumption.

The effectiveness of an intelligent lighting system highly depends on the algorithm which controls the entire system. Certain control issues in terms of system design, closed-loop system stability, output regulation are needed to be addressed while the performance indices such as energy consumption and visual preferences should also be taken into account. For instance, rapid and frequent switching of the lights on and off can occur due to unstable feedback loops, which can be disturbing to the occupants and pose possible safety concerns. The control problem could be further complicated by issues such as sensor variance, occlusion of photo-sensors, network delays in polling sensor nodes, and lighting disturbances due to daylight variations.

The deployment of robust intelligent lighting systems requires the use of distributed sensors such as motion and light sensors and power drivers that act as actuators. The distributed sensor/actuator network would enable the lighting systems to become highly responsive and be able to dynamically adapt to the users' needs while mitigating energy use. Furthermore, a lighting system should be capable of communication with other systems in the building, for example with heating and air conditioning, to manage and reduce the overall energy consumption of the building.

Lighting system components such as motion, occupancy, and ambient light sensors have been developed for a long time but they have not been able to significantly penetrate into the buildings or offices so far. High initial cost including installation, unit price, rewiring, and commissioning have been the major obstacles, especially for older buildings [5]. As a result, most of the buildings have lost the opportunity to reduce their overall energy consumption by using intelligent lighting systems.

Wireless technologies have been introduced as a promising replacement for wiring and communications in the buildings. Lower cost, less complexity, and increased flexibility are the main advantages of wireless systems when compared to wired systems. Furthermore, the emerging wireless sensor networks (WSN) technology has increased the reliability of sensor networks and actuators components. Nowadays, wireless lighting components, integrated with lighting systems, have become highly cost effective, thus making them more practical when compared to the wired networks.

The contribution in this study is twofold: we have developed a robust communication framework which is a major pre-requisite for deployment of any lighting system. The developed framework is responsible for facilitating the communication between various types of hardware such as occupancy, motion, and light sensors, as well as light actuators in the network. Daylight harvesting, motion detection and light level tuning were realized by the developed lighting system. We have also proposed a lighting control algorithm which, after integration as a part of building automation system, can satisfy the visual preferences of the users while reducing the overall amount of energy usage in the system. In open-plan environments, the proposed algorithm is capable of delivering the desired light levels for each occupant. The effectiveness of the developed lighting framework and the proposed control algorithm were also verified by two different pilot implementations.

1.2. Literature Review

Intelligent lighting control could be a very effective way of reducing the amount of energy usage in different environments (e.g., home, office). Various types of devices such as appliances, airplanes, and automobiles are becoming more intelligent in recent years. However, intelligence has not been fully applied to the lighting systems [4]. The first efforts on bringing intelligence into the lighting systems were made about twenty years ago where technologies were developed for individually controlling the output lumens of the lights. These efforts resulted in huge performance improvement only by connecting all the luminaires to a network [6] , [7], [8].

Different techniques have been studied for reducing energy usage using daylight harvesting strategies. Predefined time switching patterns and light level tuning have been developed in [9], [10] to include efficient use of daylight, consequently reducing the amount of energy consumption.

All the developed systems have proven to be effective from the energy conservation point of view. However, there are still many issues to be resolved in the field of intelligent lighting systems. Most of the available systems are not capable of providing the occupant-specific lightings levels. Instead, they usually use fairly simple algorithms to provide satisfactory light levels in the environments. Also, when there are fixture failures, the current lighting systems are not capable of performing light compensation by using other fixtures in the system. The “Plug and Play” ability in a lighting system is another important requirement to be addressed. This feature enables the users to easily add or remove light fixtures or sensors without affecting the overall system performance.

One of the first studies in the field of intelligent lighting systems were carried out by [4], in which the authors studied the problem of providing the necessary illuminance to desired locations. Their goal was to autonomously provide desired illuminance levels close to a target illuminance for all the sensors while minimizing the electrical power. In particular, the following optimization problem was defined to minimize function f given by:

$$f = \sum_{i=1}^{n} g(i) + w \sum_{j=1}^{m} Br(j), \qquad (1.1)$$

$$g(i) = \begin{cases} 0 & (Lc_i - Lt_i) \geq 0 \\ (Lc_i - Lt_i)^2 & (Lc_i - Lt_i) < 0 \end{cases}, \qquad (1.2)$$

where $g(i)$ indicates the illuminance difference between the current illuminance (Lc) and the target illuminance (Lt) and $Br(j)$ is the light luminance, n indicates the number of light sensors, and m is the number of luminaires in the system. The luminance $Br(j)$ has a linear relationship with the energy consumption of the lights. $Br(j)$ is also multiplied by a weight w which determines whether priority will be with minimizing the target illuminance or optimizing the electric power. Their proposed method was tested by a pilot implementation using fluorescent lights. This method proved to be effective in terms of reducing the amount of power consumption and delivering the desired illuminance to the sensor. It was also proven to be robust against any fixture failure or Malfunctioning. However the method suffered from a few drawbacks which might eventually lead to user dissatisfaction of the overall system. The main shortcoming of their proposed method was the lack of system's model awareness. In order to deliver the target illuminance to a sensor in a short period of time, the distance of lights and the light sensors are very important. The effect of distance between the lights fixtures and sensors was not included in the optimization function which would result in more iterations and eventually longer optimization time. Another factor which was not taken into account was the smoothness of transitions between the light levels in different iterations. Human perception of the system is an important factor which affects the lighting system performance. Frequent changes and noticeable jumps in the output light levels should be avoided as it could be uncomfortable to the users. Therefore, smooth transitions between the light levels needed to be incorporated into the system to maintain user satisfaction at all the times.

To overcome the shortcomings of the first method (i.e., increasing the speed of convergence), the same authors proposed a slightly different method in which the correlation between the luminaires and the light sensors were further taken into account [11]. To this end, based on the correlations between the luminaires and light sensors, they introduced three types of neighborhoods that were used to generate the next luminance level. Neighborhood A puts more weights to lower the luminance from current luminance to converge to target illuminance. Neighborhood B weighs the next luminance with an equally proportion to adjust the luminance. Neighborhood C puts more weight to increase the luminance intensity from current luminance.

By adopting the new rules, the luminaires which are closer to the light sensors would be actuated to satisfy the desired illuminance. Furthermore, the lights which do not have any sensors close in their neighborhood would decrease their output illuminance. The optimization function for the new method would remain unchanged, but the effect of correlation, $R(j)$, would appear in function $g(i)$ (i.e., Equation (1.3)) which indicates the error between the current and target illuminance as follows

$$g(i) = \begin{cases} 0 & (Lc_i - Lt_i) \geq 0 \\ R_j(Lc_i - Lt_i)^2 & (Lc_i - Lt_i) < 0 \end{cases}, \qquad (1.3)$$

Although incorporation of correlation factor into the optimization process improves the speed of convergence, the issues related to smooth transitions of the inputs still degrades the overall performance of their system.

Wen and Agogino proposed another lighting controller for open-plan offices [5]. They assumed that the overall lighting in an office is considered as a linear combination of the light contributions from each of the luminaires. By using a matrix representation of the illuminance model, an optimal set of d_i's (i.e., dimming levels) was selected so that each workstation is properly illuminated. Lighting energy saving and performance of the control were formulated as a linear programming problem as follows

$$min\|d\|, \text{ subject to}$$

$$Ld = T_0, \qquad (1.4)$$

$$Dimlevel_{min} \leq d \leq Dimlevel_{max},$$

where d is the vector of dimming levels, T_0 is the desired light levels, and L is the illuminance model. It is possible that the proposed optimization problem may have not a solution due to its strict constraints. Unachievable lighting conditions most likely occurs due to conflicting preferences specified by the users. In that case, the equality constraints in the optimization problem are relieved to inequality constraints to allow some tolerances [5]. Although the algorithm tries to find the optimum solution, there is no guarantee that the algorithm will converge in a limited amount of time.

There has been prior studies in which linear functions for approximation of the illuminance model were used. Guillemin [12] and Lindelhof [13] proposed predictive

models that assumed a linear relationship between the vertical illuminance and the indoor horizontal illuminance. Paulson *et al.* in 2013 proposed an inverse modeling for personalized daylight harvesting [14]. In their proposed method, a linear relationship between the illuminance measured at artificial and natural light sources and the illuminance measured at a workstation were used. They proposed a framework for using the WSN to deploy a real-time indoor lighting inverse model as a piecewise linear function of the minimum number of sensed parameter such as window light levels and dimmable lights, discretized by sub-hourly sun angles. They have found that the linear models discretized by sun angles were better able to predict the influence of daylight on the work plane illuminance.

Authors in [15] introduced the concept of illuminance matrix (I-matrix) and used it as the precise expression of the illuminance model. In their method, the I-matrix of the target working plane is obtained from several distributed light sensors using RBF (Radial Basis Function) neural networks. They further used optimization methods (i.e., genetic algorithms) and interpolations to improve the accuracy and reduce the number of sensors. Their experiments shows that their proposed I-matrix method is 30%-60% more accurate compared to the conventional control methods. Their representation of illuminance is more suitable for digital signal processing and high precision lighting control. They also reported that the I-matrix representation is more useful for places requiring a high quality of illuminance, such as operation room, cockpit, etc.

In [16], the authors suggested using a simple neural network method which can be trained to model the relationship between dimming levels as the inputs to the luminaries and the measured light levels in the environment by the light sensors. The Moore-Penrose pseudo inverse method [17] was used for the inverse modeling of the relationship between the luminous intensity and horizontal illuminance on the work planes.

Huang *et al.* [18] applied fuzzy logic theory to home automation systems. They concluded that using fuzzy control methods can reduce the electricity consumption and automatically adjust the brightness without user feedbacks.

Another work by Cabattoni *et al.* [19] also proposed a smart LED lighting controller by using the fuzzy logic theory. The objective is to control lighting level in an energy efficient way, keeping a desired light level where it is needed and reducing it to a minimum when it is not required. Their system was realized with a Proportional Integrative Derivative

(PID) law which generated the control signals based on a reference generated by a fuzzy logic block. The fuzzy controller has three inputs (i.e., ambient light, motion, LED temperature) and two outputs (i.e., reference current of the LEDs and the fan power). The method uses four membership functions of trapezoidal shape for the ambient light and temperature, two membership functions for motion, and four membership functions for both outputs. Over 50% reduction in the amount of energy usage is reported by the authors.

In [20], the authors have presented a distributed energy-saving lighting design strategy for the arrangements of a lighting network. Their target was to adaptively identify a configuration of lamps and the occupants' locations which leads to maximum energy savings in an environment. To this end, they have developed a distributed assignment strategy based on a message-passing framework where only local interactions among lamps and users are allowed for calculations and information exchange. It is claimed that the proposed method outperforms other distributed algorithms in the field of indoor lighting configurations.

Chapter 2. Communication Framework and Hardware Implementation of Proposed Lighting System

Development of a robust communication framework is a main pre-requisite for deployment of an intelligent lighting system. A lighting system requires various types of hardware such as occupancy, motion, and light sensors, as well as light actuators to work in coordination with each other. Thus, a robust distributed sensor/actuator network would be of vital importance in order to enable the lighting system to become highly responsive and dynamically adaptable to the users' preferences. The robustness of communication becomes even more important when the deployed lighting system uses a centralized type of control (i.e., lighting system in which there is at least one control unit responsible for making decisions for the entire system).

Commissioning of lighting systems is another important issue which should be taken care of at the hardware implementation stage. The need for changing settings such as node ID, node location, and other layout information for each luminaire or sensor should be feasible at any time. Thus, the designed hardware should also be capable of communication with external tools if required.

A lighting system should also be capable of communication with other systems in a building such as heating and air conditioning systems. This would enable the system to optimize the overall energy consumption in a building. The concept of connecting different devices to each other through a low power and low cost network is not new. As a matter of fact, it has been a long time that lighting components such as motion, occupancy, and ambient light sensors have been available in the market. However, they have not been deployed into the buildings or offices due to the high cost of installation, unit price, rewiring, and commissioning. As a result, many opportunities have been lost in buildings to reduce the overall energy usage and efficiency through intelligent automation systems.

Nowadays, wireless technologies are becoming more and more popular and excellent candidates for replacing wired communication in buildings. Lower cost and complexity, when compared to wired technologies, and increased flexibility are the main

advantages of wireless systems. The emerging wireless sensor networks (WSN) technology has also increased the reliability of sensor networks and actuator components. Nowadays, wireless lighting components integrated with lighting systems have become cost-effective and practical solutions for building installations.

Until recently, the TCP/IP protocol has been the most successful protocol in the field of communication networks which has enabled communication across millions of computing devices worldwide. Using the TCP/IP protocol for connecting devices in a Building Automation System (BAS) such as sensors, actuators has been an interesting idea. However, internet technology was considered too heavy for the low-power and low-cost devices used in BAS. The main reason which prevents the use of TCP/IP protocol in a BAS is the TCP/IP's high protocol overhead for transferring data. This will increase the power consumption of BAS devices and eventually lower their life cycle. In the following section, an overview of the available IEEE wireless standards is presented along with their performance in a BAS.

2.1. IEEE Wireless Standards

IEEE wireless standards are a set of rules, protocols, and techniques defined by the IEEE LAN/WAN standard committee (IEEE 802) [21] for implementing wireless local area networks (WLAN). The protocols and services defined by this committee are restricted to the two lower layers (Data link layer and physical layer) in the OSI network reference model [22]. More specifically these protocols are defined solely for the Physical layer (PHY) and Medium (Media) Access Control (MAC) sub layer of Data link layer. Figure 2.1 illustrates the two widely used network layer representations, the OSI and Kurose-Forouzan models [23], [24], and their relationship with the IEEE 802 standard defined for wireless network applications. The MAC sub layer and PHY layer together provide the necessary channel access mechanism and hardware transmission technology for communicating between different nodes in a wireless network.

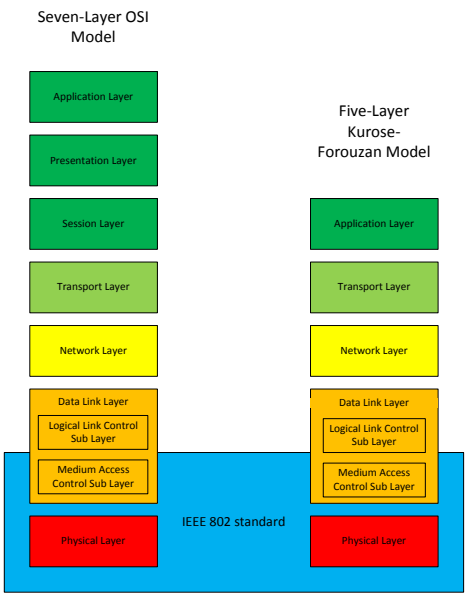

Figure 2.1. IEEE 802 standards restricted to lower layers on OSI and Kurose-Forouzan models.

Currently, there are three IEEE standards, namely IEEE 802.11, IEEE 802.15.1 and IEEE 802.15.4, which are widely used in today's wireless applications. In the following sub sections, these three standards and their applications in building automation systems are briefly introduced.

2.1.1. IEEE 802.11 or Wi-Fi

IEEE 802.11 standard, commonly known as Wi-Fi [25], is a set of low tier, terrestrial network technologies for data communication [26]. Wi-Fi standard operates in the 2.4 GHz and 5 GHz Industrial, Science and Medical (ISM) frequency band. It also has many different variations such as IEEE 802.11 a/b/g/n [26]. Wi-Fi is a high power, high data rate, and wide range wireless network standard which is widely used in personal computers, video game consoles, and smartphones. A Wi-Fi enabled device can connect to the internet through a wireless network access point.

2.1.2. IEEE 802.15.4 or ZigBee

IEEE 802.15.4 is a low tier, ad hoc, terrestrial wireless standard which was developed to meet the need for simple, low power, and low cost wireless communication [26]. This standard is commonly known as ZigBee [27]; although ZigBee has more features

in supporting the higher layers in the OSI model. In the past couple of years, this standard has received a lot of attention in the field of wireless sensor networks. The first generation of ZigBee standard operates in the 2.4 GHz ISM band, but the second and third generation of the ZigBee standard operates in Sub-1 GHz frequency bands, mostly to avoid its potential interference with Wi-Fi which operates in the same band [28].

2.1.3. IEEE 802.15.1 or Bluetooth

IEEE 802.15.4 standard is a group of low tier, ad hoc, terrestrial network protocols which is the basis of the Bluetooth technology [26]. It is designed for small and low cost devices which usually have low power consumption [26]. Bluetooth technology [29] operates in the 2.4 GHz ISM band as well, but uses a frequency hopping scheme [30] to avoid interference with other wireless technologies. The Bluetooth technology has three different classes which differ in their range of coverage. Class 1 covers up to 100m, while class 2 and class 3 cover 10m and 1m, respectively [26]. Bluetooth low energy (BLE) [29] is also a newly introduced version of the Bluetooth standard which aims at lowering power consumption compared touts earlier versions.

2.1.4. Modes of Operation

There are two different modes of operation defined for wireless networks: Ad hoc and infrastructured [26]. An infrastructured wireless network is a type of network that needs at least one base station in which all of the nodes in the network communicate with or through that station. Usually, the base station also provides internet access for the network. Base stations usually have fixed locations. A very common example of an infrastructured network is the Wi-Fi network, in which all of the devices are required to communicate with an access point. The major disadvantage of an infrastructured network is its dependency on the base station. In majority of the cases, if the base station in an infrastructured network stops working, the entire network would stop working as well. In contrast to the infrastructured network, the Ad hoc networks can be formed anywhere without a central base station. In the Ad hoc networks each node can talk to the other nodes without having to talk to a base station in between. Table 2.1 illustrates common IEEE wireless standards with their associated modes of operations.

Table 2.1. Modes of operations for different IEEE wireless standards (Table taken from [26]).

Standard	Ad hoc	Infrastructured
802.11a/b/g/n	Yes	Yes
802.15.1	Yes	No
802.15.4	Yes	No
802.15.6	Unknown	Unknown

2.1.5. Network Topology

Choosing an appropriate network topology plays a vital role in the process of network design. Inappropriate selection of a network topology for a specific application may result in waste of time and energy. Even after installation, it might further require a lot of troubleshooting to resolve possible network problems. Bluetooth and BLE support the ad-hoc piconet topology [31]. This topology is very similar to a star topology, where a master node in a piconet controls multiple slave devices. The slave devices can only communicate with the master node and are not able to communicate with each other directly. It is also possible that a slave device would participate in two different piconets. The number of devices in each piconet is limited to 8. Figure 2.2 shows the typical topology of Bluetooth and BLE technologies.

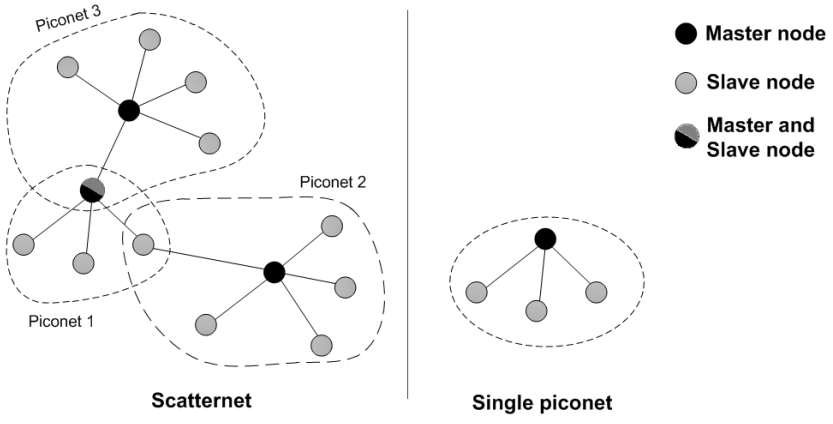

Figure 2.2. A typical Bluetooth topology. Image taken from [29].

There are two main disadvantages associated with the piconet topology. In each piconet, if the master stops working due to some internal problems, all its associated slave nodes will also be disconnected from the network. Furthermore, if the failed piconet was an intermediate piconet belonging to a larger network, then the rest of piconets would also be disconnected from the base station. Another disadvantage of piconet topology is its limited scalability. It would be almost impossible to scale up the piconet topology for a large number of nodes without any latency problems.

In the mesh topology, a message sent out by any nodes in the network can take different paths from the source to the destination. This topology is more suitable for networks with a large number of nodes. It can cover a wide range of area by using routers in the network structure as well. Also, a node failure would not affect the entire network since there exist many different paths for the nodes to communicate. The ZigBee standard supports mesh network topology. There are three types of nodes in a ZigBee network; Co-ordinator, routers and end devices. A coordinator is the most capable devices in the ZigBee network. It can communicate with the routers and end devices in the ZigBee network. It also acts as a gateway to communicate with other networks. Routers in the ZigBee network can pass messages from one node to another, which are also capable of making local decisions. There are also end devices in a ZigBee network which have the lowest capabilities. They are usually used to relay data from sensors and actuators to higher network layers. Figure 2.3. illustrates a typical ZigBee network topology. One of the main drawbacks of mesh topologies is their protocol overhead. The ZigBee networks usually have low data transfer rate mainly due to their routing protocol overheads [31].

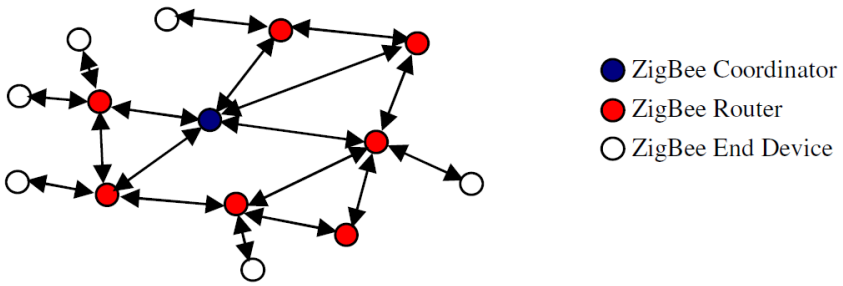

Figure 2.3. A typical ZigBee topology. Image taken from [31].

2.1.6. Frequency, Data Transmission Rate, and Range

The wireless technologies described in the previous subsections differ in many aspects, including their frequency of operation, network topology, coverage range, and power consumption. These dissimilarities directly influence their application in the market. Table 2.2 briefly compares the various types of IEEE wireless standards, their frequency of operation, data transmission rate and range of operation. The IEEE 802.15.6 mentioned in the table is an upcoming high frequency technology designed for wireless body area network (WBAN) [26]. However, not much information has been released about this technology so far. Table 2.3 summarizes the differences between three low power technologies mostly used in the field of wireless sensor networks.

2.1.7. Modulation and Interference

Many of the wireless communication devices operate in the unlicensed 2.4GHz ISM band. Thus, interference is another important issue that has to be taken care of at the time of technology selection. The IEEE 802.11 and IEEE 802.15.1 protocols both operate in the 2.4GHz ISM band whereas the IEEE 802.15.4 protocol supports three different frequency ranges, i.e., the 868, 915 MHz frequency ranges and the 2.4GHz high frequency ISM band. The IEEE 802.15.4 protocol uses binary phase shift keying (BPSK) modulation in 868/915 MHz band and quadrature phase shift keying (QPSK) modulation in 2.4GHz [31]. Figure 2.4 shows the relationship between the signal to noise ratio (SNR) and bit error rate (BER) for three different modulations used by these standards.

Table 2.2. A comparison between frequency, data transmission rate and range of different wireless technologies (Table taken from [26]).

Standard	Frequency	Data Transmission Rate	Range	Type
802.11a	5 GHz	54 Mbps	120m	LAN
802.11b	2.4 GHz	11 Mbps	140m	LAN
802.11g	2.4 GHz	54 Mbps	140m	LAN
802.11n	2.4/5 GHz	248 Mbps	250m	LAN
802.15.1	2.4 GHz	3 Mbps	100m	PAN
802.15.4	868/915MHz, 2.4GHz	40 kbps, 250 kbps	75m	PAN
802.15.6	1 THz	> 1 Gbps	10m	BAN

Table 2.3. Detailed comparison of three well-known low power wireless technologies. Table taken from [31].

	Bluetooth	ZigBee	BLE
Application	Computer and accessory devices, computer to computer and computer with other digital devices	Home control, building automation, industrial automation, home security, medical monitoring	Sport and fitness products, watches, remote control and healthcare devices
Frequency band	2.4, 2.48 GHz	868MHz, 902-928MHz, 2.4-2.48GHz	2.48 GHz
Topology	Ad-hoc piconets	Ad-hoc, star, mesh	Ad-hoc piconets
Scalability	Low	High	High
Range	10 meters	100 meters	10 meters
Maximum data transfer rate	3 Mbps	20 Kbps, 40 Kbps, 250 Kbps	1 Mbps
Power consumption	100 mW	30 mW	10 mW
Access method	TDMA	CSMA/CA	TDMA, FDMA
Encryption	128-bit encryption E0 stream cipher	128-bit AES block cipher (CTR, counter mode)	12bit AES block cipher (CCM mode)
Modulation	GFSK, 2PSK, 8PSK	BPSK (868/928MHz) QPSK (2.4 GHz)	GFSK
Robustness	16-bit CRC	16-bit CRC	24-bit CRC

It can be inferred from this figure that ZigBee modulation is generally about 7 to 18 dB better than Bluetooth and Wi-Fi modulations [28]. This could be interpreted as a 2-8 times increase in the range of coverage for the same energy per bit in all the standards, or more reliable transmission at the same range [28].

As mentioned earlier, the Bluetooth technology uses a frequency hopping scheme for its data transmission on the 2.4GHz ISM band.

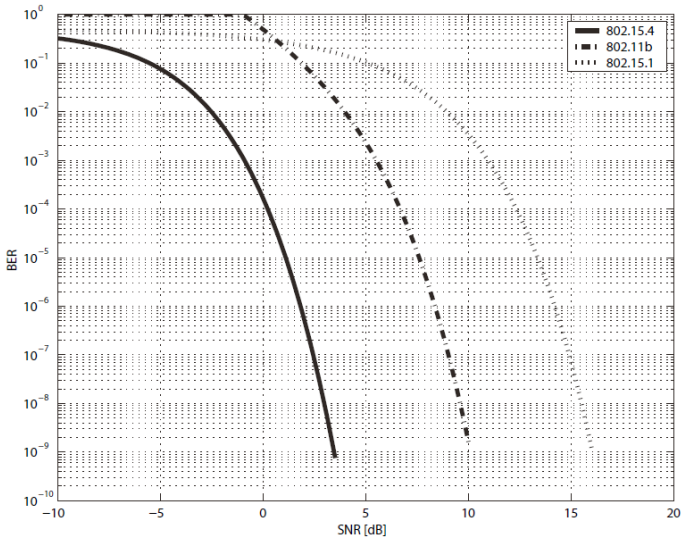

Figure 2.4. Bit error rate in an additive white Gaussian noise for three different IEEE standards. Figure taken from [28].

This method has reduced the possibility of interference with the higher power technologies up to a very good extent. As a result, there has been not much interference reported between the Bluetooth with Wi-Fi or even ZigBee. In this regard, one should also inspect the interference between the Wi-Fi and ZigBee technologies, both of which operate in the 2.4MHz frequency band. Figure 2.5 shows a case study carried out by [28] in which two nodes are communicating through IEEE 802.11b/g and two other nodes are communicating through IEEE 802.15.4. Figure 2.6 illustrates the frame error rate of IEEE 802.15.4 when it has interference with the IEEE 802.11b. It could be inferred from the figure that the damage to the communication is very severe when the two standards are working in the same frequency range. However, by shifting the IEEE 802.15.4 frequency, the amount of interference starts to degrade. Authors in [28] concluded that a minimum of 7 MHz frequency difference is required between the IEEE 802.11 and IEEE 802.15.4 to work properly in the same environment. Also, it is necessary to point out that the effect of IEEE 802.15.4 interference on an ongoing IEEE 802.11 communication is negligible [28]. Due to the large interference effect of IEEE 802.11 standard on the IEEE 804.15.4, the second and third generations of the ZigBee compliant chips operate on the Sub-1 GHz frequency band. Working in lower frequency bands increases the range of operation. It is also less affected by the multipath propagation and absorption effects. But these benefits are all achieved at the cost of higher energy consumption and a larger size of the antenna.

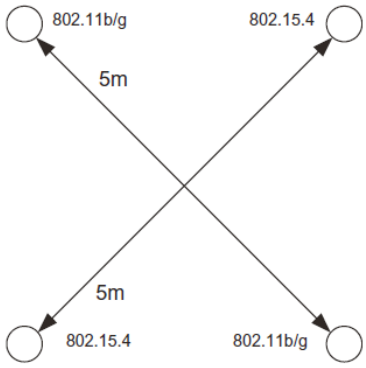

Figure 2.5. A very simple example of two network standards interfering each other. Image taken from [28].

2.2. Technology Selection for the Proposed Lighting System

Various high level wireless protocols and stacks are available in today's market such as Zigbee, ANT, Z-wave, and Bluetooth. Based on the target applications, each of the available protocols are in compliance with at least one of the IEEE wireless standards. The IEEE 802.15.1 (e.g., Bluetooth and BLE) standard enables direct connection with a variety of user interface devices such as mobile phones, laptops, and tablets. But its application as a wireless

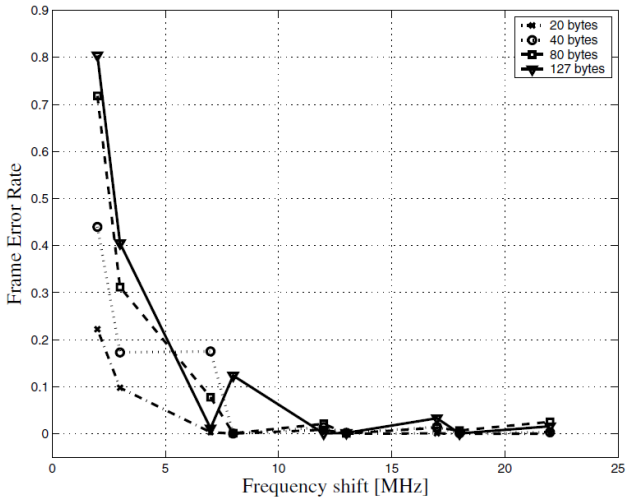

Figure 2.6. IEEE 802.15.4 frame error rate for different packet size when interfered by IEEE 802.11b network. Image taken from [28].

network framework in large scale installations has limitations with respect to the network configuration, size, and power consumption. On the other hand, IEEE 802.15.4 compliant technologies have advantages including low power consumption, relatively simple structure, and support for large network installations which make them ideal choices in the field of home automation. By considering the pros and cons of each standard in home automation systems, one of the IEEE 802.15.4 compliant were chosen as the communication framework for the proposed lighting system.

Among IEEE 802.15.4 compliant wireless protocols, ZigBee [27] is the most well-known protocol which has recently received a lot of attention and become very popular in the field of wireless sensor networks. ZigBee-based products are widely used in applications such as light switches, electrical meters, and home displays. The first generation of ZigBee standards operates in the 2.4 GHz ISM band, but the second and third generations operate in Sub-1 GHz frequency bands, mostly to avoid its potential interference with Wi-Fi.

JenNet is another protocol developed by Jennic/NXP for low-power short-range wireless networking applications based on the IEEE 802.15.4 specifications [32]. JenNet supports star, tree, and linear network topologies, and provides self-healing functionality for robust communication [32]. The low-power and low-cost characteristics of Jennic wireless chips provide good opportunities for developing home automation systems with reduced power consumption. Followings are some of the features provided by the JenNet stack [32] which would be vital in the implementation stage of a lighting system:

- Support for network size up to 500 nodes,
- Automatic route formation and repair,
- Network load balancing to avoid data throughput congestion,
- Network re-shaping to reduce network depth,
- Sleeping end devices for extended battery life,
- Over the air download.

The compliance of Jennic technology with IEEE 802.15.4 and additional features provided by its stack significantly simplify the hardware implementation stag. Thus the Jennic wireless technology was chosen as the main communication framework for the proposed

lighting system. This includes all the inter-network communications between the sensors, actuators, routers, and gateways in the developed lighting system.

2.3. Architecture and Components of the Proposed Lighting System

In the proposed lighting system, each hardware component such as sensor, actuator, control unit and any other device in the network is considered to be a wireless node capable of communicating with other nodes through the selected wireless technology. The Jennic protocol has the capacity of addressing up to 65535 nodes in a single network [32]. However, there are only three general types of nodes in a network: co-ordinators, routers, and end devices. Each type of node has its own role in the network structure. Meanwhile, it may also perform additional tasks at the application level, independent of its role at the network level. For instance, a network of Jennic devices measuring ambient light levels may have a light sensor application in each node, irrespective of whether they are end devices, routers, or a co-ordinator. The architecture of the network and different components in the developed lighting system with their roles at the network level are briefly described in the following subsections.

2.3.1. Protocol Stack and Network Topology

The JenNet stack supports tree, star, and linear network topologies along with self-healing functionality for robust communication [32]. In the developed lighting system, the tree topology was chosen as the primary network topology. A tree topology consists of a coordinator to which other nodes are connected as follows:

- The coordinator is linked to a set of routers and end devices
- A router may then be linked to more routers and end devices.

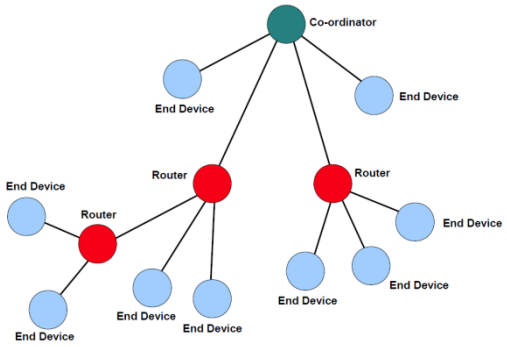

Figure 2.7. Topology of the proposed lighting system. Image taken from [32].

2.3.2. End Devices

The main task of an end device at the network level is to send and receive messages. The end devices cannot relay messages and cannot allow other nodes to connect to the network through them. Sensors and actuators are two main components in the developed lighting system operating as end devices.

2.3.2.1 Sensors

In the developed lighting system, the sensor components include at least one motion detector, one ambient light sensor, and a wireless chip. These components have the capability to communicate with their local parents (in a tree network topology structure) and transfer data to upper levels. They are also capable of performing the actions requested by their local parents.

2.3.2.2 Light Control Units

The light control unit acts as a driver for LED luminaires in the developed lighting system. An LED driver is the power supply for the LED, very similar to ballasts for fluorescent or HID (High intensity discharge) lights. Drivers with dimming capability could dim the luminaire light output over the full range from 100% to 0%. They can dim LEDs by reducing the forward current, performing pulse width modulation (PWM) voltage control, or more sophisticated methods [33]. The developed light control unit uses the PWM method for dimming the LEDs. With PWM, the frequency could range from hundred modulations per second to as high as hundreds of thousands of modulations per second.

Thus the LED output would appear to be continuously lighted without flicker. Along with driving the LEDs, light control units have other responsibilities such as performing regular safety tests, temperature monitoring, reporting the amount of energy consumption, and detecting any failure or malfunctioning in the luminaire.

2.3.3. Routers

Network routers are used for regenerating their received signals. If a node cannot reach other nodes or its parent due to long distance problems, then a router could be placed in between to enhance the communications. Routers are also useful for extending the network capacity. As the number of nodes starts to grow in a large network, a combination of routers and coordinators would help to accommodate more nodes in the network.

2.3.4. Co-ordinator

All Jennic networks must have one (and only one) co-ordinator, irrespective of the network topology. In the Tree and Mesh topologies, the co-ordinator is the top (root) node in the network. The main tasks of the coordinator at the network layer are:

- Selecting the frequency channel to be used by the network,
- Initializing the network,
- Allowing other devices to join to the network.

2.3.5. Gateway

In general, a Gateway is an inter-networking device which facilitates the communication of two or more different networks when they are using different networking protocols. A gateway can be implemented in many different ways. A computer program can perform the job of a gateway. It can also be implemented completely in hardware or a combination of software and hardware. An embedded gateway is a low power embedded circuitry which is highly capable in the communications aspect. It typically consists of protocol translators, signal translators, impedance matching devices, and fault isolators. In the developed lighting system, the gateway is responsible for translating the Jennic

communication protocol to the Ethernet protocol, hence sending the necessary data over the internet.

Gateways are also responsible for long range communication within the network devices. Low power wireless networking protocols such as ZigBee or Jennic are usually classified as low-range networking protocols. These protocols are inherently not capable of long-range communications (i.e., inter-floor communications) between the networking elements. In the case of long-range networking, gateways are responsible for the task by using a long range protocols such as Wi-Fi or Ethernet. Therefore, to develop a lighting system for a large building, gateways are required in order to establish a connection between all networking elements in different sections of the building.

2.3.6. User Interface

A web-based graphical user interface (GUI) was designed for the users to be able to interact with the developed lighting system. Real-time and offline monitoring of data, scheduling, daily and monthly reports, power consumption tracking of the lighting system, and manual control of each node were among the provided features for the web-based interface. Further details on the developed GUI are presented in Chapter 4.

Chapter 3. Proposed Algorithm for Intelligent Lighting Control

Visual comfort and energy saving are two main aspects of an intelligent lighting system. Modern lighting systems can achieve major energy savings by utilizing appropriate lighting control strategies. However, the users' lighting preferences and visual comfort have been generally overlooked in conventional systems. Human perception has always been an important factor affecting the overall performance of a lighting system. Not much of the studies carried out in this field have focused on satisfactory delivery of the desired illuminance to the users. Not to mention that frequent changes or noticeable jumps in the output light levels could also be uncomfortable for the users. The entire lighting control procedure could become even more complicated by issues such as sensor variance, occlusion of photo-sensors, network delays in polling sensor nodes, and lighting disturbances due to daylight variations. In this section, we present a lighting control algorithm which can be integrated with a building automation system to satisfy the visual preferences of the users while reducing the amount of energy usage due to lighting. The proposed algorithm is capable of delivering the desired light levels for each occupant in open-plan environments. Apart from this goal, other important control issues such as output regulation, system stability and performance criteria such as energy consumption were taken into account. To this end, the entire lighting system is considered as a multiple-input, multiple-output closed-loop control system with the following characteristics:

1. The control inputs are the applied power to LED luminaires,
2. The reference inputs are desired light levels at arbitrary sensor locations,
3. The system outputs are the light levels on the selected locations,
4. The daylight is disturbance to the system.

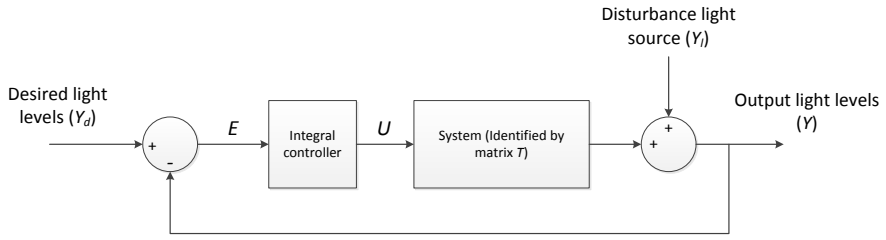

Figure 3.1. Block diagram of the proposed control algorithm.

3.1. System Modeling

A block diagram of the proposed control method is shown in Figure 3.1. As illustrated in this figure, the plant in the closed-loop control system is represented by a $m \times n$ matrix T, which indicates the relationship between the input and the output signals of the control system. More specifically, the elements of matrix T represent the relationship between the input power to the luminaires in the system and the illuminance at the sensor level. The elements of matrix T are dependent on physical properties of the system such as geometry and color. Representation of the system model by a constant matrix T implies that the inputs and outputs of the lighting system are assumed to be linearly related to each other. This way of modeling could be in fact an accurate one for lighting systems utilizing LED luminaires. Experiments carried out in [34] show that the input power of an LED and its total output luminous flux could be linearly related within a certain range. From [34], an equation which relates the output luminous flux (φ) of an LED luminaire to its input electrical power is given by

$$\varphi = NE_0\{[1 + k_e(T_a - T_0)P_d + k_e k_h(R_{jc} + NR_{hs})P_d^2]\}. \quad (3.1)$$

This formula integrates the photometric, electrical and thermal aspects of the LED luminaire together. The term E_0 is the rated efficacy of the LED at the rated temperature T_0; R_{jc} and R_{hs} are the thermal resistances of the junction and heat sink of the LED respectively; k_e is the relative rate of reduction of efficacy with increasing temperature; and k_h is a constant representing the portion of LED power that turns into the heat. Equation (3.1) can be rewritten in the form of:

$$\varphi = \alpha_1 P_d - \alpha_2 P_d^2, \tag{3.2}$$

where α_1 and α_2 are two positive coefficients [34]. The positiveness of α_1 and α_2 is due to the constant k_e being negative. By increasing the input power from zero, the output luminous flux of the LED increases almost linearly because the second term is negligible when P_d is small. But as P_d increases, the second term in (3.2) will reduce the output luminous flux significantly as it is proportional to the square of P_d [34]. The operation point P_d^*, corresponding to the maximum output luminous flux, can be obtained from the following formula:

$$P_d^* = -\frac{[1+k_e(T_a-T_0)]}{2k_e k_h(R_{jc+}NR_{hc})}. \tag{3.3}$$

Thus, we could expect that for any input power less than P_d^*, the output luminous flux of the LED is almost linearly related to the input power. The validity of this argument was also confirmed by experiments carried out in [34] as shown in Figures 3.3 and 3.4. It would be ideal to operate the LEDs at their optimum operating power, i.e., any power below the P_d^*. Thus, in any lighting system which uses LEDs as its lighting fixtures and with the operating power for each luminaire less than P_d^*, the output luminous flux could be estimated as a linear function of its input power. That is to say, for any LED luminaire in the system we have

$$\varphi_i = \alpha_i P_{di}. \tag{3.4}$$

where φ_i is the output luminous flux of $i-th$ LED, P_{di} is the input power to the LED, where α_i is the coefficient which relates the luminous flux of the LED to its input power. The relationship between the luminaires' flux and the illuminance in the lighting system should also be considered. An extensive analysis of this relationship could be found in [35]. By using the inverse square law [36], in a lighting system with n number of point light source with luminous -

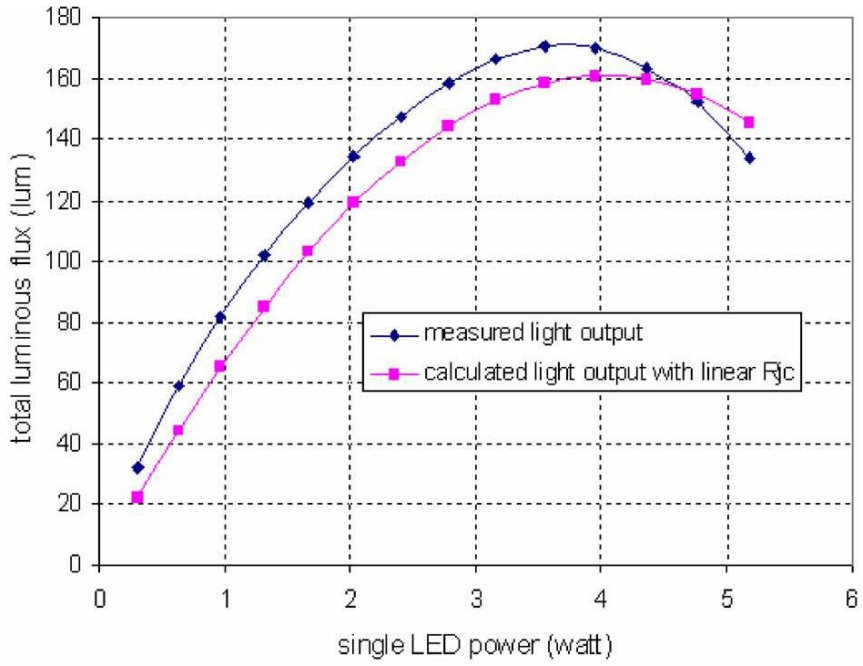

Figure 3.2. Calculated and measured total luminous flux versus lamp power for two Luxeon 5W LEDs mounted on heatsink with thermal resistance of 10 ◦C/W. Image by [34].

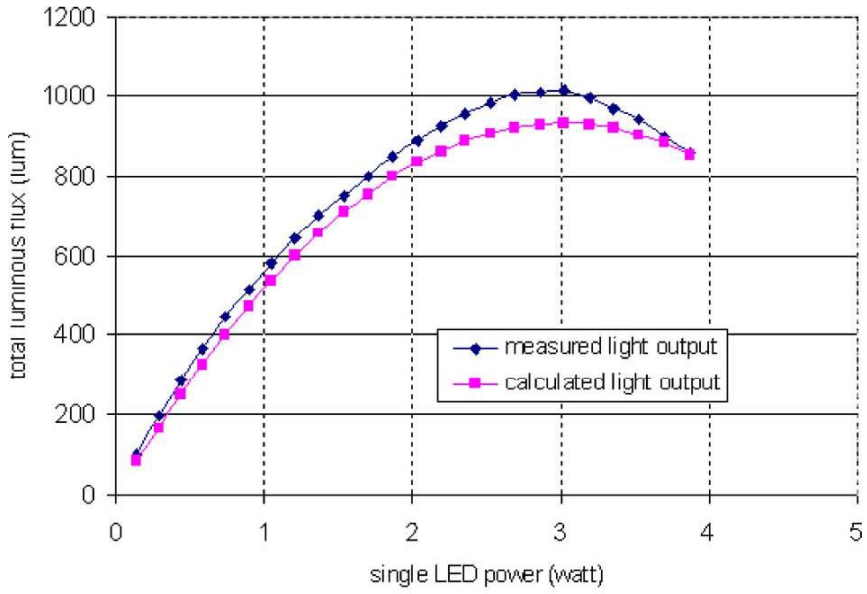

Figure 3.3. Calculated and measured total luminous flux versus lamp power for two CREE 3W LEDs mounted on heatsink with thermal resistance of 4.5 ◦C/W. Image by [34].

flux given by $\varphi_1, \varphi_2, \ldots, \varphi_n$ and m light sensors, the illuminance of the $j-th$ sensor is calculated from

$$E_j = \frac{1}{4\pi}\sum_{i=1}^{n}\frac{\varphi_i}{d_{ij}^2}, \tag{3.5}$$

where d_{ij} indicates the distance between the $i-th$ light sensor and $j-th$ light source. By extending the above formula to all the light sensors in the system we have

$$\begin{bmatrix} E_1 \\ E_2 \\ . \\ . \\ . \\ . \\ . \\ E_m \end{bmatrix} = \frac{1}{4\pi}\begin{bmatrix} \frac{1}{d_{11}^2}, \frac{1}{d_{12}^2}, \ldots\ldots\ldots\ldots\ldots\ldots\ldots\ldots, \frac{1}{d_{1n}^2} \\ \frac{1}{d_{21}^2}, \frac{1}{d_{22}^2}, \ldots\ldots\ldots\ldots\ldots\ldots\ldots\ldots, \frac{1}{d_{2n}^2} \\ \\ \\ \\ \\ \\ \\ \frac{1}{d_{m1}^2}, \frac{1}{d_{m2}^2}, \ldots\ldots\ldots\ldots\ldots\ldots\ldots\ldots, \frac{1}{d_{mn}^2} \end{bmatrix}\begin{bmatrix} \varphi_1 \\ \varphi_2 \\ . \\ . \\ . \\ . \\ . \\ \varphi_n \end{bmatrix} \tag{3.6}$$

Equation (3.6) represents a linear relationship between the illuminance and the luminous flux in a lighting system with point light sources. By estimating each LED luminaire in the lighting system as multiple point light sources and by assuming that all the LEDs luminaires are working at their optimum operating range, we could further combine (3.4) and (3.6) as follows

$$\begin{bmatrix} E_1 \\ E_2 \\ . \\ . \\ . \\ . \\ . \\ E_m \end{bmatrix} = \frac{1}{4\pi}\begin{bmatrix} \frac{1}{d_{11}^2}, \frac{1}{d_{12}^2}, \ldots\ldots\ldots\ldots\ldots\ldots\ldots\ldots, \frac{1}{d_{1n}^2} \\ \frac{1}{d_{21}^2}, \frac{1}{d_{22}^2}, \ldots\ldots\ldots\ldots\ldots\ldots\ldots\ldots, \frac{1}{d_{2n}^2} \\ \\ \\ \\ \\ \\ \\ \frac{1}{d_{m1}^2}, \frac{1}{d_{m2}^2}, \ldots\ldots\ldots\ldots\ldots\ldots\ldots\ldots, \frac{1}{d_{mn}^2} \end{bmatrix}\begin{bmatrix} \alpha_1 P_{d1} \\ \alpha_2 P_{d2} \\ . \\ . \\ . \\ . \\ . \\ \alpha_n P_{dn} \end{bmatrix}$$

$$= \frac{1}{4\pi}\begin{bmatrix} \frac{\alpha_1}{d_{11}^2}, \frac{\alpha_2}{d_{12}^2}, \dots\dots\dots\dots\dots\dots\dots\dots, \frac{\alpha_n}{d_{1n}^2} \\ \frac{\alpha_1}{d_{21}^2}, \frac{\alpha_2}{d_{22}^2}, \dots\dots\dots\dots\dots\dots\dots\dots, \frac{\alpha_n}{d_{2n}^2} \\ \vdots \\ \frac{\alpha_1}{d_{m1}^2}, \frac{\alpha_2}{d_{m2}^2}, \dots\dots\dots\dots\dots\dots\dots\dots, \frac{\alpha_n}{d_{mn}^2} \end{bmatrix} \begin{bmatrix} P_{d1} \\ P_{d2} \\ \vdots \\ P_{dn} \end{bmatrix} = T_{m\times n} \begin{bmatrix} P_{d1} \\ P_{d2} \\ \vdots \\ P_{dn} \end{bmatrix}. \quad (3.7)$$

From (3.7) it follows that the illuminance outputs in a lighting system with LED luminaires are linearly related to the input power of the LEDs, assuming that the LEDs are working within their optimal operating range. In reality there are many factors which could affect the ultimate behavior of a lighting system. In practice, the LED luminaires in a lighting system are not point light sources. Instead, they usually consist of multiple LED strings placed in parallel with each other in one package. Another factor which may cause inaccuracy in the modeling of a lighting system could be the effect of light reflections on the illuminance. This effect could vary from very small changes to very large ones depending on the structure of the environment, material texture, and location of the objects in the installation site. Nevertheless, the linearity assumption of the illuminance model is still a very good estimation of the behavior of the real system. The uncertainty of the lighting model could be further compensated by the feedback control algorithm.

3.2. Proposed Control Method

Before applying any feedback control scheme to the lighting system, a system identification test is carried out to obtain the system model from measuring the real data. The identification process is covered in Chapter 4. For now, let us assume that the system model can be represented by a $n \times n$ square matrix with the elements known to the control algorithm. Based on this assumption, the entire control process could be described as follows

1. The users choose their desired light levels and initialize the system.
2. Each ambient light sensor reads its current light level and sends its value back to the central control unit over the wireless network.

3. Once all ambient light levels and system model are known, new dimming levels for lighting fixtures are calculated by utilizing a proper control scheme and sent out to the luminaires over the network.
4. All the luminaires will change their output light levels to the new values.
5. By repeating steps 2 to 4, the proposed lighting system continuously senses the light levels in the environment with the objective of minimizing deviations from the desired values.

By sensing the ambient light levels continuously over the time, the system can also respond to any unexpected changes in the environment immediately such as sensor or fixture malfunctioning, sensor occlusion, and daylight variations.

As pointed out before, the goal of the proposed lighting system is to bring the illuminance close to the target illuminance for each sensor, while trying to minimize the energy usage in the system. To make the proposed lighting system robust and reliable, the above mentioned objectives should be properly formulated. By considering the system block diagram shown in Figure 3.4, let us define the following state variable

$$X(t) = \int_0^t E(\lambda) d\lambda, \tag{3.8}$$

where $X(t) = [x_1(t), x_2(t), \dots, x_n(t)\,]$ represents the state vector and $E(t) = [e_1(t), e_2(t), \dots, e_n(t)\,]$ represents the error vector of the system. Then one can write

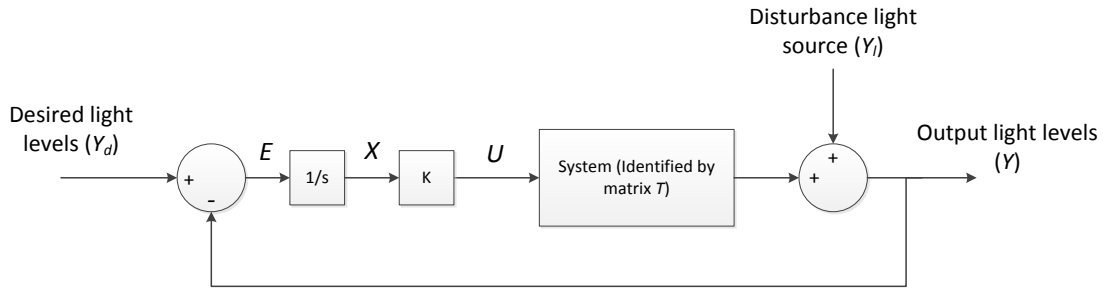

Figure 3.4. Block diagram of the proposed lighting control algorithm.

$$E(t) = Y_d - Y(t) = -TU(t) + Y_d - Y_l \Rightarrow \quad (3.9)$$

$$\dot{X}(t) = -TU(t) + (Y_d - Y_l). \quad (3.10)$$

Utilizing the state feedback $U = KX$ results in

$$\dot{X}(t) = -TKX(t) + Y_d - Y_l, \quad (3.11)$$

$$Y(t) = TKX(t) + Y_l. \quad (3.12)$$

Taking the Laplace transform of both side in (3.11) results in

$$sX(s) - X(0) = -TKX(s) + \frac{Y_d - Y_l}{s},$$

$$X(s)(s + TK) = X(0) + \frac{Y_d - Y_l}{s},$$

$$X(s) = \frac{X(0)}{s+TK} + \frac{Y_d - Y_l}{s(s+TK)}. \quad (3.13)$$

Equation (3.13) is the solution of the $X(t)$ in the Laplace domain. By recalling the Laplace inverse transforms [37]:

$$L^{-1}\left(\frac{b}{s+a}\right) = be^{-a} \quad (3.14)$$

and

$$L^{-1}\left(\frac{1}{s}F(s)\right) = (u * f)(t), \quad (3.15)$$

where $u(t)$ is the step function and $(u * f)(t)$ is the convolution of $f(t)$ and $u(t)$, the solution of $X(t)$ in the time domain is obtained as follows

$$X(t) = e^{-TKt}X(0) + \int_0^t e^{-TK(t-\tau)}(Y_d - Y_l)d\tau. \qquad (3.16)$$

By assuming a constant disturbance/reference (i.e., $Y_d - Y_l = const.$), the second term in (3.16) can be simplified as follows

$$\int_0^t e^{-TK(t-\tau)}(Y_d - Y_l)d\tau = \left(\int_0^t e^{-TK(t-\tau)}\,d\tau\right)(Y_d - Y_l) =$$

$$\left(\int_t^0 e^{-TK\sigma}\,d\sigma\right)(Y_l - Y_d) = [(TK)^{-1}e^{-TK\sigma}]_t^0 \times (Y_d - Y_l) =$$

$$(TK)^{-1}[I - e^{-TKt}](Y_d - Y_l).$$

Thus (3.16) can be simplified as follows

$$X(t) = e^{-TKt}X(0) + (TK)^{-1}[I - e^{-TKt}](Y_d - Y_l). \qquad (3.17)$$

Based on (3.8), the error term can be obtained as follows

$$E(t) = (-TK)e^{-TKt}X(0) + (TK)^{-1}[(TK)e^{-TKt}](Y_d - Y_l) =$$

$$E(t) = (-TK)e^{-TKt}X(0) + e^{-TKt}(Y_d - Y_l). \qquad (3.18)$$

Assuming that the TK matrix is positive-definite, we have

$$E(t) \to 0, \qquad as \quad t \to \infty.$$

Thus, by choosing an appropriate matrix K which would result in positive-definiteness of TK, the closed-loop system error would converge to zero as the time approaches infinity. Equations (3.11) and (3.12) also represent the state and output equations of the closed-loop control system. As a multiple-input multiple-output linear time

invariant system, positive-definiteness of matrix TK (i.e., negative-definiteness of matrix $(-TK)$) would also result in asymptotic stability of the closed-loop system [38].

3.3. Choice of Optimal Feedback Gain

As pointed out in Section 3.1, the objective of an intelligent lighting system is twofold: minimizing the amount of energy consumption in the system and accurately delivering the target illuminance chosen by the users. To better define the problem, a quadratic performance index is used as follows

$$J = \frac{1}{2}\int_0^\infty (E^T QE + U^T RU)dt. \tag{3.18}$$

In (3.18), E represents the system error, U represents the input power to the system, and Q and R are the cost weight for each term. Minimizing the performance index J is equivalent to fulfilling both objectives in the lighting system. The above optimal control problem is concerned with operation of a dynamic system at minimum cost. In general, optimal control methods cope with the problem of finding a control law for a given system such that a certain optimality criterion is achieved. Linear Quadratic Regulators (LQR), a more abstract framework in this field, deals with cases where the system dynamics are described by a set of linear differential equations along with a quadratic function performance index. Based on the LQR theory in optimal control [39], the solution to the minimization of for the following cost function

$$J = \frac{1}{2}\int_0^\infty (X^T QX + U^T RU)dt, \tag{3.19}$$

where $X(t)$ is the trajectory of the continuous time system $\dot{X}(t) = AX(t) + BU(t)$, is the linear time-invariant state feedback given by

$$U(t) = -R^{-1}B^T PX(t) = KX(t). \tag{3.20}$$

where P is the positive-definite solution of the *Riccati equation* [40]:

$$PA + A^T P + Q - PBR^{-1}B^T P = 0. \tag{3.21}$$

The LQR controller is essentially a static state feedback control law. Thus the steady state of the LQR is not offset error free when the system is subject to a constant disturbance or a constant reference input [41]. When disturbances, or nonzero reference inputs are present, the standard LQR problem must be modified so that the controller has a right structure [41]. To this end, let us define our new performance index as

$$J = \frac{1}{2}\int_0^\infty (E^T QE + V^T RV)dt \tag{3.22}$$

where Q and R are positive-definite and V is the derivative of input vector U, i.e.,

$$\frac{dU(t)}{dt} = V(t).$$

From (3.9), it follows that

$$E(t) = Y_d - Y(t) = -TU(t) + Y_d - Y_l \Rightarrow$$

$$\dot{E}(t) = -T\dot{U}(t) = -TV(t). \tag{3.23}$$

Equation (3.9) is now reformulated as a standard LQ problem with $A = 0$ and $B = -T$ in (3.23). Thus the linear time-invariant feedback which minimizes the performance index given by (3.22) can be written as follows

$$V(t) = -R^{-1}B^T PE(t)$$

where P is obtained by solving the *Riccati equation* given in (3.21). Also, the value of $U(t)$ is given by

$$U(t) = \int_0^t V(\lambda)d\lambda = \int_0^t -R^{-1}B^T PE(\lambda)d\lambda =$$

$$-R^{-1}B^T P\int_0^t E(\lambda)d\lambda = -R^{-1}B^T PX(t) = KX(t)$$

The main idea in this development is to use the time derivative of $U(t)$ in the performance index. In a conventional LQR problem, $U(t)$ is penalized, as a result of which $U(t)$ converges to zero and the cost function remains bounded. By including the time derivative of $U(t)$ in the performance index, $U(t)$ does not need to converge to zero but to any arbitrary value [41].

The blocks surrounded by dotted lines in Figure 3.5 represent a new plant with state equation $\dot{X}(t) = -TU(t)$ and arbitrary output equation $Y(t) = X(t)$ (i.e., $A = 0, B = -T, C = 1, D = 0$) for the closed-loop control system. Note that the formula in (3.23) is the derivative of the state equation of the new plant. We could further simplify our system block diagram with a proportional state feedback K as depicted in Figure 3.6. Based on the LQR theory, the LQR controller always yields stable closed-loop feedback if the pair (A, B) is controllable and Q is positive-definite [39]. In this case, K would make the system asymptotically stable. The controllability of pair (A, B) can be further assessed by investigating the rank of $n \times nm$ controllability matrix given by

$$R = [B\ AB\ A^2B\ \ldots\ A^{n-1}B]. \qquad (3.24)$$

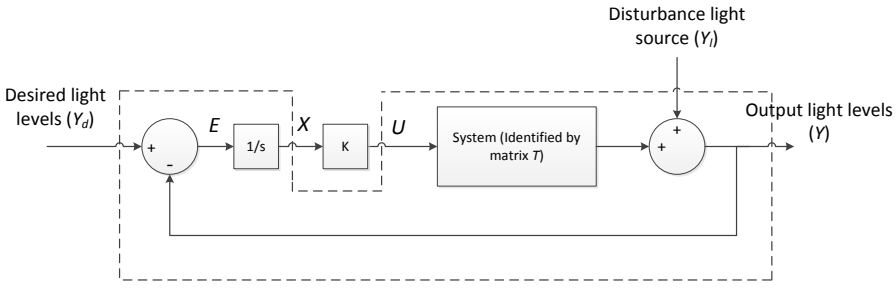

Figure 3.5. Block diagram of the proposed intelligent lighting control algorithm. Dotted lines shows the new plant in the system for LQR optimization.

Pair (A, B) is controllable if and only if the controllability matrix is full rank (i.e., $Rank(R) = n$). This condition could be further assessed by obtaining the system model. For now, by assuming controllability of the system, the optimum value of K can be obtained by solving the *Riccati equation* given by (3.21). Assuming $A = 0$, $B = -T$, $Q = qI$ and $R = rI$, (3.21) can be written as

$$qI - \frac{1}{r}P(-T)I(-T^T)P = 0.$$

Matrix P can then be obtained as follows

$$PTT^TP = rqI \Rightarrow$$

$$TT^T = P^{-1}rqIP^{-1} \Rightarrow$$

$$\frac{1}{rq}TT^T = P^{-2} \Rightarrow$$

$$P = \sqrt{rq}(TT^T)^{-1/2}. \qquad (3.25)$$

Hence, the state feedback coefficient K is obtained as follows

$$K = -R^{-1}B^TP = -(rI)^{-1}(-T)^T\sqrt{rq}(TT^T)^{-1/2} \Rightarrow$$

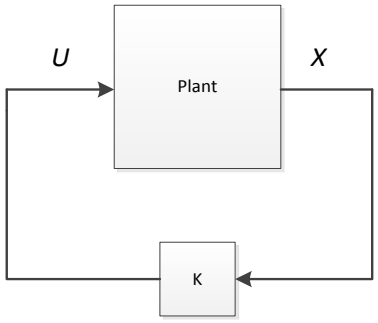

Figure 3.6. Simplified block diagram of the system with the proportional state feedback.

$$K = \sqrt{\frac{q}{r}} T^T (TT^T)^{-1/2}. \qquad (3.26)$$

3.4. Systems with Non-square Matrix Models

In the previous section, it was assumed that the plant matrix T is a $n \times n$ square matrix. This implies that the number of inputs and outputs are the same (i.e., equal number of light fixtures and light sensors). In situations where the number of light sensors is not equal to the number of light fixtures, which is indeed a very possible scenario, the system model is not a square matrix any more. To analyze such scenarios, three distinct cases are considered:

1. When the number of inputs (i.e., light fixtures) is smaller than the number of outputs (i.e., sensors illuminance), we have an under-actuated system. In this case, the system generally does not have a solution because there are more equations than unknowns.
2. When the number of inputs is equal to the number of outputs, the system has always a mathematical solution as long as $det(T) \neq 0$.
3. When the number of inputs is larger than the number of outputs, we have an over-actuated system with multiple solutions in general.

In the case where the number of luminaires is more the number of light sensors, a possible solution would be to replace the non-square system model with a square model since there exist sufficient number of light fixtures to satisfy the desired illuminance.

Let assume that T is a full row-rank matrix (i.e., $Rank(T) = m$) with basis vectors given as $\underline{b}_1, \underline{b}_2, \ldots\ldots, \underline{b}_m$, then for a non-square system model where T is a $m \times n$ matrix and $n > m$. Hence, we have

$$TU = \left[\underline{t}_1, \underline{t}_2, \ldots\ldots \underline{t}_n\right] \begin{bmatrix} u_i \\ . \\ . \\ . \\ u_n \end{bmatrix} =$$

$$= \left[\underline{b}_1, \underline{b}_2, \dots \dots \dots, \underline{b}_m\right]_{m\times m} \begin{bmatrix} \gamma_{11}, \gamma_{12}, \dots \dots, \gamma_{1n} \\ . \\ . \\ . \\ \gamma_{m1}, \gamma_{m2}, \dots \dots, \gamma_{mn} \end{bmatrix} \begin{bmatrix} u_i \\ . \\ . \\ . \\ u_n \end{bmatrix}_{n\times 1} =$$

$$B_{m\times m} \begin{bmatrix} \gamma_{11}, \gamma_{12}, \dots \dots, \gamma_{1n} \\ . \\ . \\ . \\ \gamma_{m1}, \gamma_{m2}, \dots \dots, \gamma_{mn} \end{bmatrix} U_{n\times 1} =$$

$$= B_{m\times m}\Gamma_{m\times n}U_{n\times 1} = BW,$$

where

$$\Gamma = \begin{bmatrix} \gamma_{11}, \gamma_{12}, \dots \dots, \gamma_{1n} \\ . \\ . \\ . \\ \gamma_{m1}, \gamma_{m2}, \dots \dots, \gamma_{mn} \end{bmatrix},$$

is a unique coefficient matrix, describing T in terms of basis vectors and $W = AU$. Therefore, when the system model is not square, the non-square model can be replaced with a square model in which

$$TU = BW. \qquad (3.27)$$

We can obtain the optimum feedback coefficient K_B in a similar way as matrix K was obtained in square models. The only difference would be replacing the non-square matrix T with square matrix B in (3.27). The input vector U can also be found as

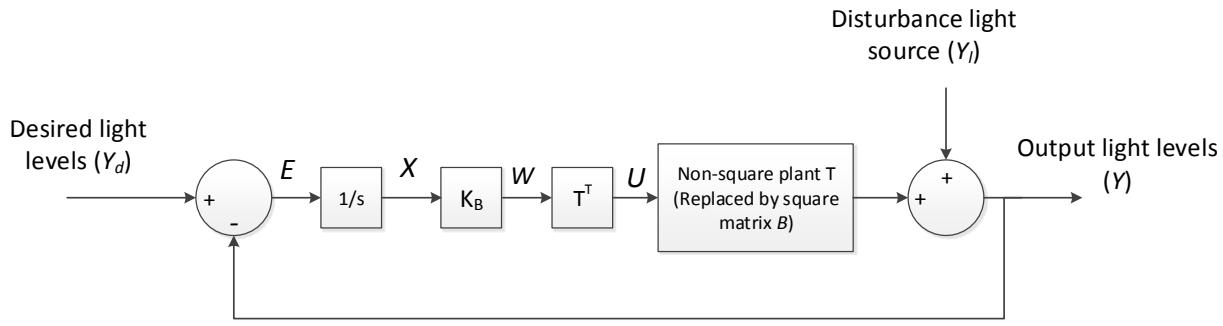

Figure 3.7. Non-square system model solution for the proposed lighting control algorithm.

$$\Gamma_{m\times n}U_{n\times 1} = W_{m\times 1} \Rightarrow$$

$$U = \Gamma^{\dagger}W + \left(I - \Gamma^{\dagger}\Gamma\right)\gamma_{n\times 1} \qquad (3.28)$$

where $\Gamma^{\dagger}$ is the pseudo-inverse of matrix Γ and $\gamma_{n\times 1}$ is any arbitrary vector. There would be infinite solutions for the matrix U, but the minimum-norm solution is given by

$$U = \Gamma^{\dagger}W. \qquad (3.29)$$

The general solution for any arbitrary non-square system (i.e., any number of lighting fixtures and light sensors in the system) can be obtained from the following steps:

1- For any non-square system, we find the basis vectors of T and form the square matrix B.
2- By Using T and B we find $m \times n$ matrix Γ.
3- By replacing T with B in (3.26), we find the optimum feedback gain for the system.
4- Input vector U can be further obtained from (3.28).

Chapter 4. Experimental Evaluation of the Developed Lighting System Platform

This chapter presents the implementation and experimental steps carried out to evaluate the performance of the developed lighting infrastructure. In particular, experimental results obtained during one year pilot deployment of the developed lighting infrastructure are presented for a facility located in North Vancouver, BC. Daylight harvesting, motion detection, and light level tuning were different strategies explored using the developed system during the test period. Furthermore, various features including real-time and offline monitoring of the luminaires, power consumption of individual luminaires, and instantaneous manual control of each light were also examined during the test period that are presented in this chapter as well.

4.1. Pilot Implementation of Developed Wireless Lighting System

The distributed wireless lighting system discussed in Chapter 2 was deployed in the dining room of a care center located in Lyn Valley, North Vancouver. The room dimensions are 53 ft. × 23 ft. containing 8 dining tables and one shared work space. Originally 21 compact florescent lamps (CFL) were physically wired together in the dining room which could only be turned on/off by switches located at both ends of the room. This configuration is referred to as the “base installation” in the rest of this chapter. All 21 CFLs were retrofitted with 7 dimmable 35W CREE22 Troffer LEDs [42]. All the LED fixtures were equipped with the wireless-enabled light control unit. Seven sensor units consisting of ambient light and motion sensors were placed on the ceiling of the dining room. The wireless units were pre-programmed to operate in a self-configuring network mode upon the powering up. The developed wireless structure ensures that the actuation commands and sensors data propagate through the network accordingly.

The dining room was located near the courtyard in the building with a very large window facing the outside light, making it suitable for using the daylight harvesting strategy. The pilot implementation prevents energy waste by turning on the lights when

someone enters or stays in the room and then automatically turns them off when there is no activity in the room for a pre-defined period of time. Ambient light sensors also helped in reducing the amount of energy consumption by forcing the luminaires to go off when there was enough light during the daylight hours. To minimize unnecessary fluctuations in the output lights of the fixtures, a new set of dimming levels were triggered only if the variation in the ambient light was more than 10% of its current level. Based on feedback from the residents during the test period, the changes in the output light were very smooth and almost unnoticeable to the occupants.

A web based graphical user interface (GUI) was also developed and provided to the users in the care center. Real-time and offline monitoring of each luminaire status, power consumption tracking of the individual luminaire, and instantaneous manual control of each light were among the provided features of the web-based interface. Allowing the users to override the light settings and status could be an effective way for the system to learn about the users' lighting preferences. It has been shown in the literature that the users always demand a certain amount of control, no matter how smart the system could be [43] [44]. Therefore, an overriding mechanism that could record the user's lighting preferences were also incorporated in the system. Another feature that proved to be very useful during the test period was the scheduling ability offered by the web-based GUI. This feature enabled the users to schedule the luminaires to provide fixed outputs for any arbitrary period of time during each day. In this mode, all the luminaires will provide fixed output lights regardless of feedback coming from motion and ambient light sensors.

The time series of the luminaires activities during one day of operation is shown in Figure 4.1. The original sampling period was 5 seconds which was further scaled to fit in a one-day period plot. These figures present the activity of three luminaires during 24 hours, starting from 12:00AM to 11:59PM in December 1st, 2012. Each luminaire was set to turn off if there were no activity around it for at least thirty seconds. The zero power consumption shown in the time series are representative of the periods in which the luminaires were turned off due to no activity detection. Figures 4.1.a and 4.1.b represent the activities of two luminaires placed in the hall way of the dining room, hence showing more activities compared to the third luminaire (shown in Figure 5.1.c) which was placed on the corner of the dining room. The times between 11:00AM to 1:00PM and 4:30PM to 6:00PM are the lunch and dinner times in the care center and the luminaires are prescheduled to fixed output during these periods. Samples of hourly power consumption

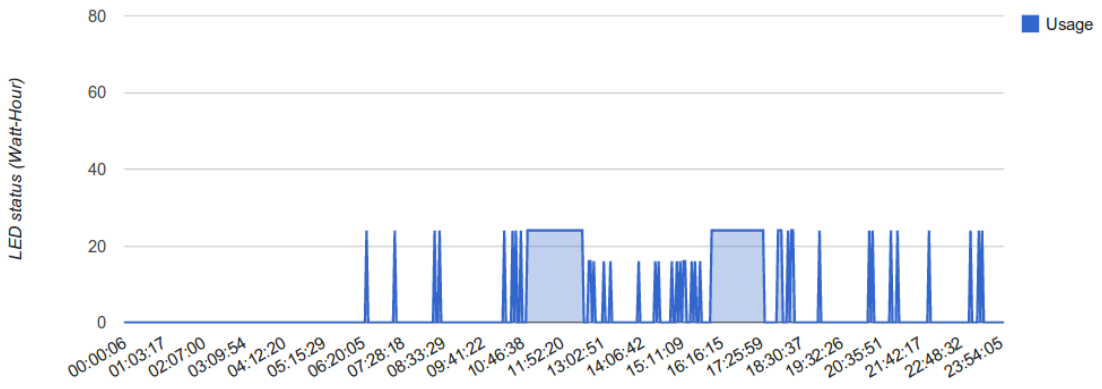

a

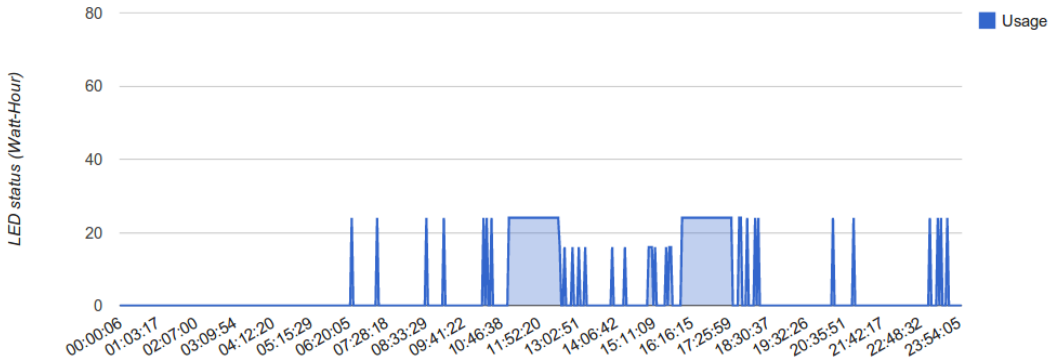

b

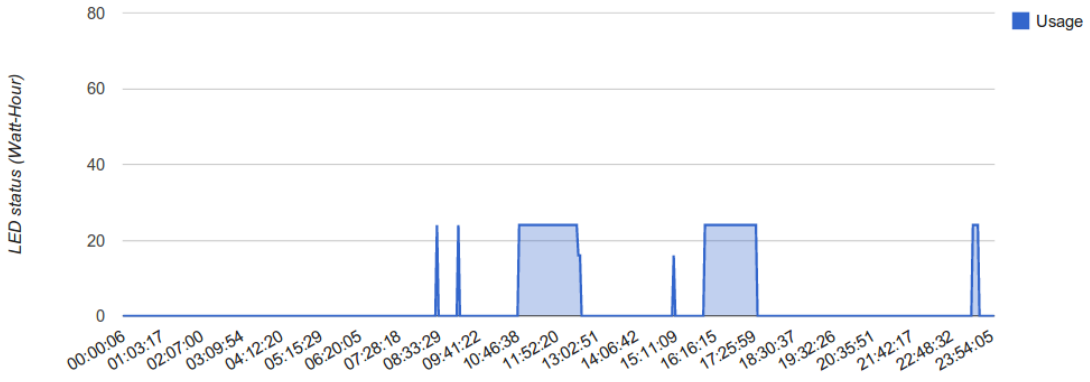

c

Figure 4.1. Time series of luminaires activity in one day during the pilot implementation. Luminaires in (a) and (b) are placed in the hall way while (c) is placed at the corner of the room.

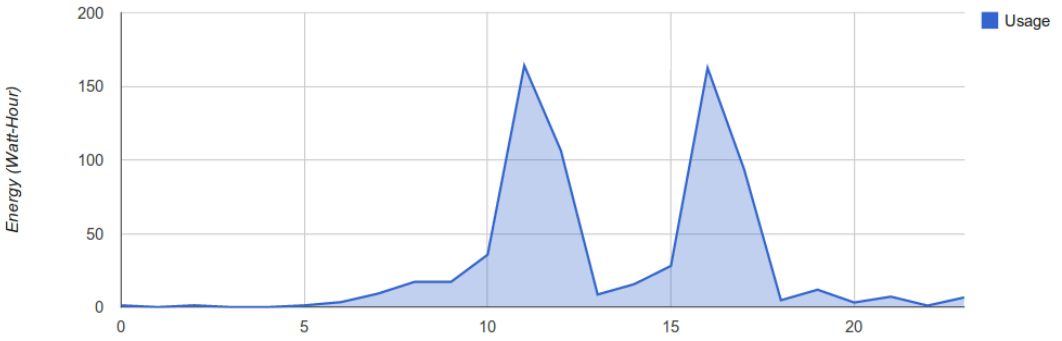

a

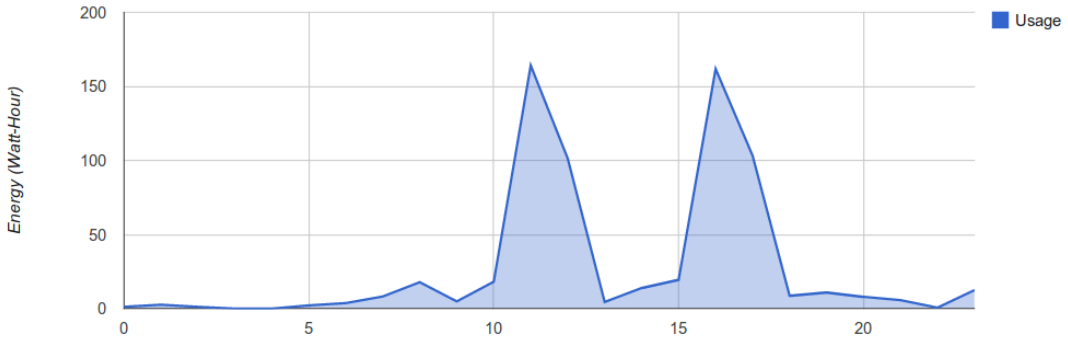

b

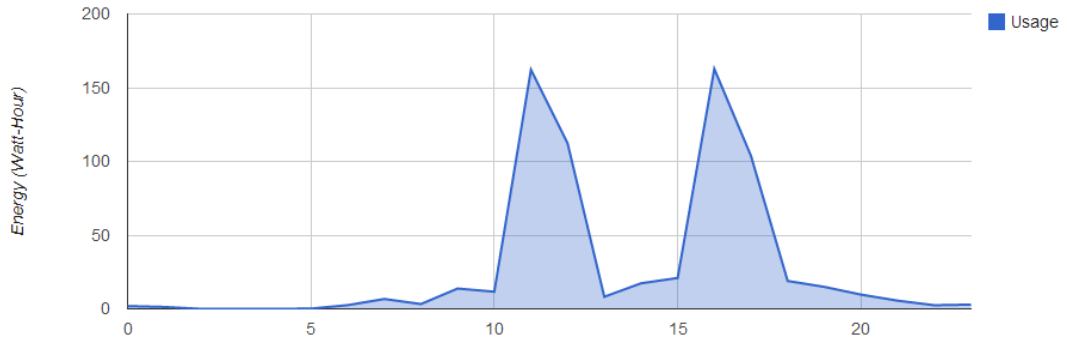

c

Figure 4.2. Hourly power consumption of the lighting system during three different days during the pilot implementation. (a) September 1st, (b) October 1st, (c) November 1st in 2012. Note that the maximum power consumption periods happen during the lunch and dinner times when the luminaires are prescheduled to deliver a fixed light output.

of the deployed lighting system during three different days are depicted in Figure 4.2. By sampling the activity of the system for every 5 seconds, the total power consumption of the entire system in each hour could be calculated as follows

$$Total\ power\ per\ an\ hour = \sum_{for\ all\ the\ luminaires} \frac{active\ seconds}{3600} * 35watts.$$

It can be concluded from these figures that the maximum daily power consumption periods happen during the lunch and dinner times in the care center when the luminaires are prescheduled to deliver a fixed light output. To better estimate the amount of energy savings during the pilot implementation, the daily energy usage by the deployed lighting system was also recorded and compared to the base installation. Figures 4.3, 4.4 and 4.5 illustrate the amount of energy usage for base and new installations in three different months. The replacement ratio was assumed to be 1 to 1 (i.e., each CFL is replaced by one LED luminaire) in order to better demonstrate the effect of deployed lighting system. The daily energy usage for the base installation consisting of 42W CFLs can be obtained as follows

$$Base\ installation\ daily\ energy\ usage = 7 * 42\ watts * 24\ hours = \ 7056\ watt - hour.$$

The above calculation is based on the fact that the CFL luminaires in the base installation are not dimmable and work at their full output all the times. The percent of energy savings for the selected months were 89.89%, 89.55% and 88.87%, respectively. The amount of energy savings during different months of the year was almost the same. This is due to the fact that the care center users preferred to use the same scheduling scheme for all the days during the test period. Feedback from ambient light sensors were essential for the system to effectively optimize the fixtures' output light levels based on the level of ambient light. Figure 4.6 shows the time series of illuminance values read by one of the ambient light sensors in the deployed lighting system during the first day of May, June and December of 2012. The effect of outside light is distinguishable on the illuminance values read by the installed ambient light sensor.

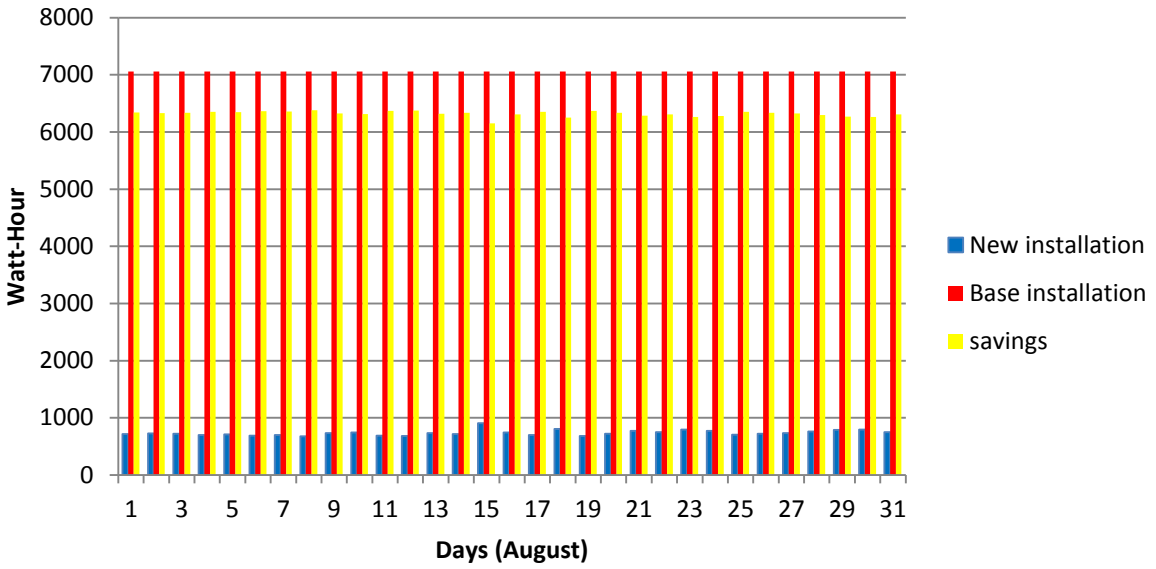

Figure 4.3. Comparison between the power consumption of the base installation and the new installation during August, 2012.

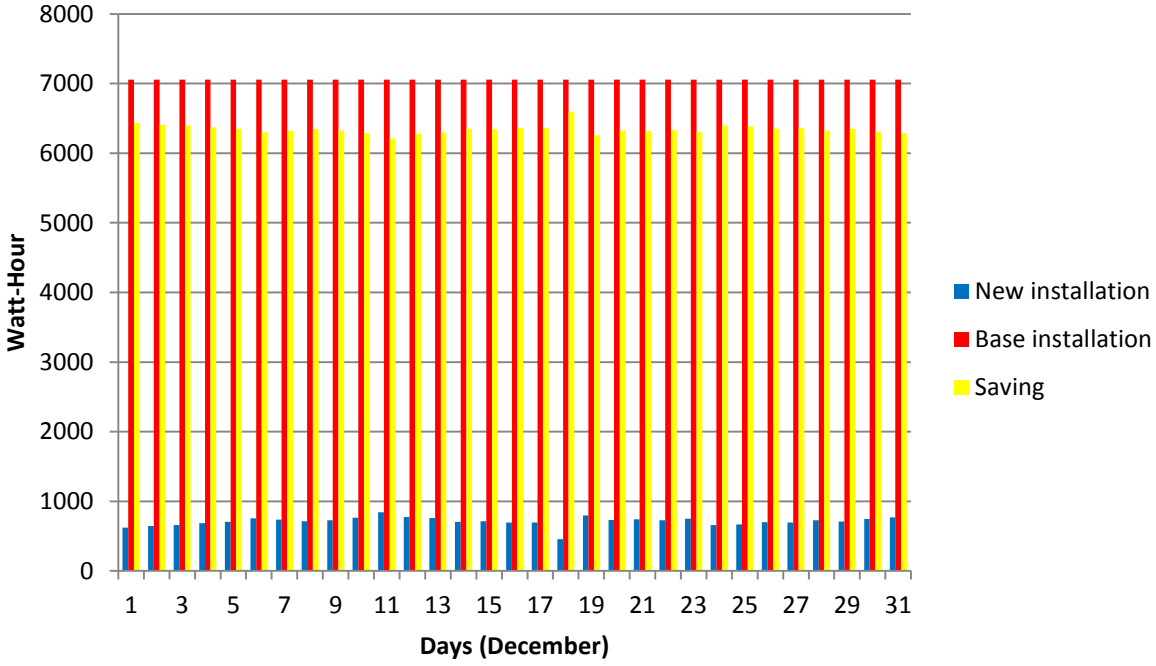

Figure 4.4. Comparison between the power consumption of the base installation and the new installation during December, 2012.

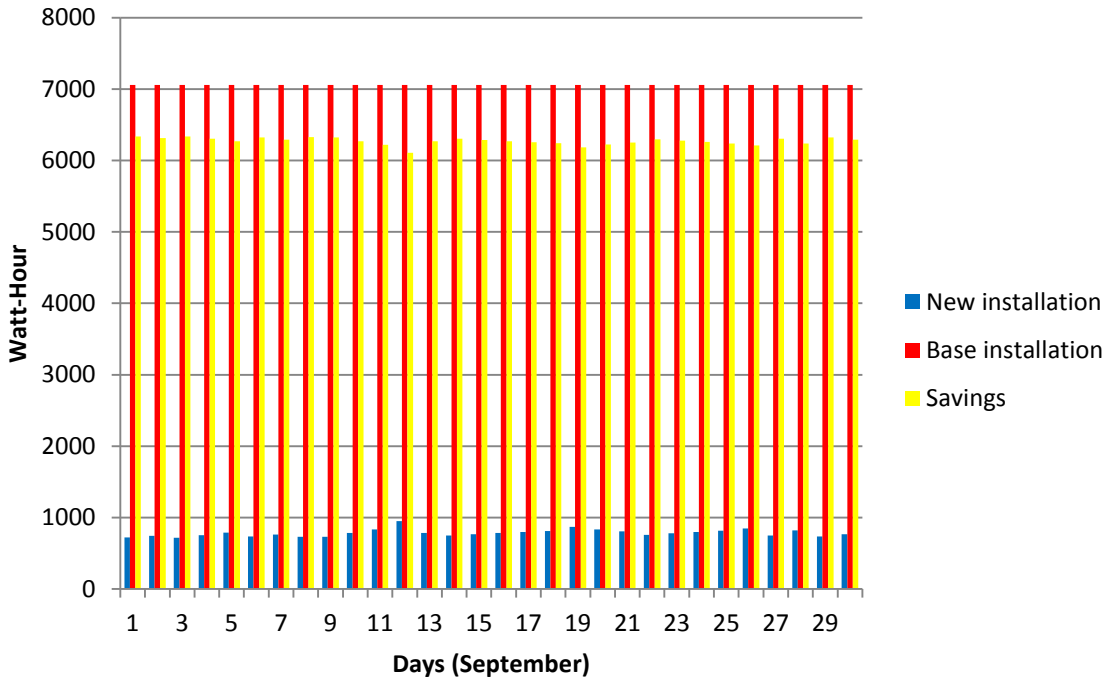

Figure 4.5. Comparison between the power consumption of the base installation and the new installation during September, 2012.

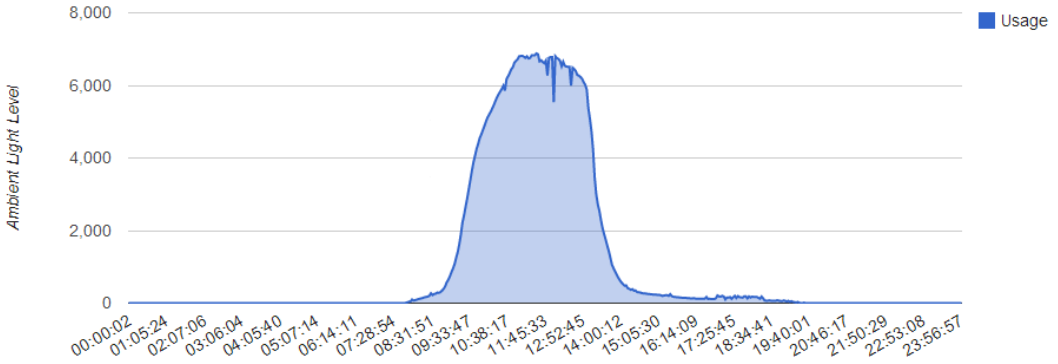

a

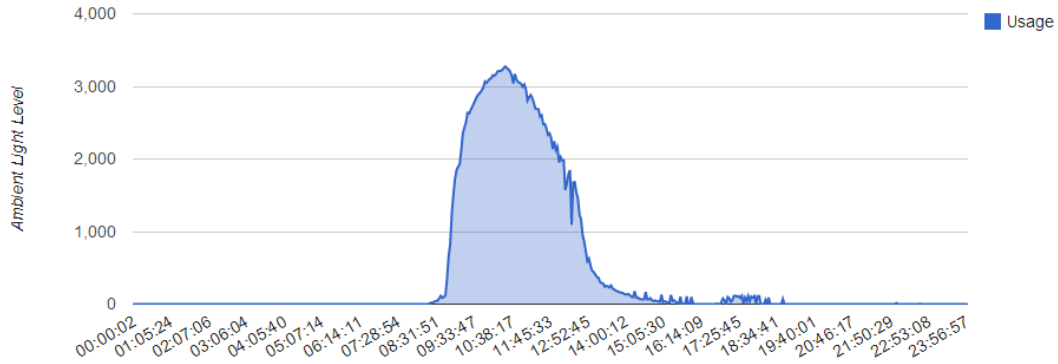

b

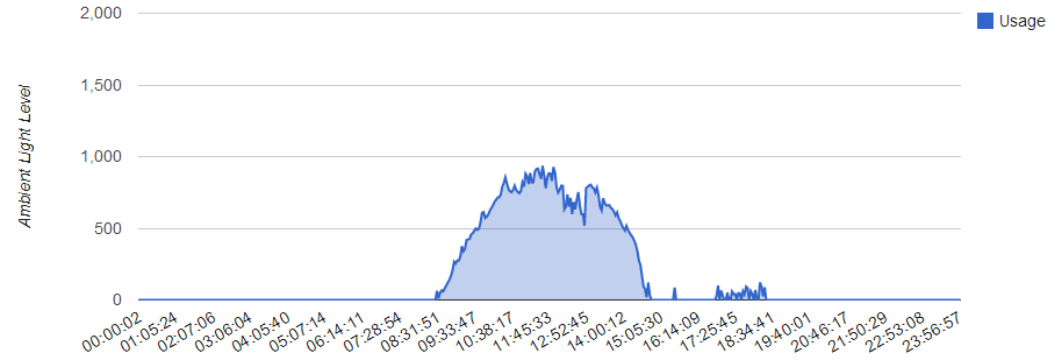

c

Figure 4.6. Time series of illuminance values read by one of the ambient light sensors in the deployed lighting system during the first day of (a) May, (b) June and (c) December of 2012.

Chapter 5. Pilot Implementation of Proposed Lighting Control Algorithm

The effectiveness of the proposed lighting control algorithm was simulated and verified on a proof-of-concept laboratory setup. The testbed was a $1 \times 1 \times 1\ m^3$ wooden box containing two LED luminaires and two ambient light sensors as shown in Figure 5.1. To minimize the effect of outside light on the sensor readings, the inside of the box is completely isolated from the outside light when the box is closed. The isolation from outside light will help to accurately identify the system model (i.e., identifying the relationship between the input power to the luminaires and the illuminance at the sensor level without any disturbance) during the system identification test. Light sensors and LED luminaires were chosen from the available off-the-shelf products in the market. Xeleum XCO-100 [45] motion and daylight harvesting sensor was selected to be incorporated in our system (Figure 5.2). The two LED luminaires were H042T 84W LED panel lights from BDS industrial solutions [46]. The proposed lighting control algorithm was implemented on a desktop PC using the MATLAB/Simulink environment, which was also responsible for coordinating the data communication between the actuators and ambient light sensors.

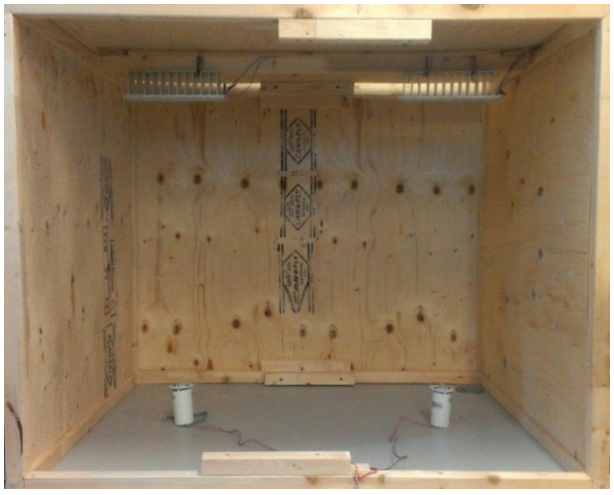

Figure 5.1. A wooden box containing two LED luminaires and two ambient light sensors used as the test bed for verifying the effectiveness of proposed control algorithm.

A MSP430 micro controller [47] was used to facilitate the data transmission between the PC, sensors, and the actuators for driving the lights. The communication between the Simulink and MP430 micro controller was made possible through the serial port of the PC.

The entire control process could be briefly described as below:

1. The user provides the controller with the desired light level for each ambient light sensor in the box as a reference input to the control system.
2. The controller reads current light level of each ambient light sensor.
3. Having the light levels and system model in hand, based on the proposed control algorithm, new dimming levels for the luminaires are calculated and sent to the light drivers through RS232 serial port.
4. Luminaires will adopt the new values received from the control unit.
5. By repeating steps 2 to 4, the proposed lighting system continuously senses the light levels in the environment and tries to minimize the error of the control system and satisfactory deliver the desired values.

Figure 5.2. Xeleum XCO-100 [45] used as the ambient light sensor in the test bed.

5.1. System Identification

Recalling from Chapter 3, the relationship between the input power to the luminaires and the illuminance was described by a linear model. It should be mentioned that a linear model was proposed with the assumption of an empty environment. In reality, uncertainties would be present due to unaccounted light reflections from different furniture in the room, wall, etc. While different factors such as furniture type, size, and arrangement in the room may have impacts on the system model, these effects could be considered as a part of the system's model uncertainty and would be minimized by the feedback system.

The very first step in implementing the proposed algorithm is to identify the system model. In terms of the number of inputs and outputs, our test setup represents a 2×2 system, where the number of luminaires and the number of sensors are equal to each other. This system could be modeled by a 2×2 matrix T where:

$$T = \begin{bmatrix} t_{11} & t_{12} \\ t_{21} & t_{22} \end{bmatrix},$$

and t_{ij} represents the relationship between the $i-th$ luminaire and the $j-th$ light sensor. To obtain the relationship between the luminaires and the light sensor in the test setup, two series of experiment were carried out. Let us call the LED luminaire and ambient light sensor placed on the left hand side of the wooden box, LED1 and ALS1, respectively, and ones on the right hand side as LED2 and ALS2. In the first experiment, a range of different dimming levels starting from 0 to 100% were fed into the LED1, meanwhile the light levels read by ALS1 and ALS2 were recorded. During this experiment the LED2 was turned off for the entire test, hence excluding the effect of its output light on the reading values of the ambient light sensors. The second experiment was carried out in a very similar fashion, only this time dimming levels were fed to the LED2, while the LED1 was kept off. The data obtained in both experiments are shown in Tables 5.1 and 5.2, respectively. These data sets were also plotted in Figure 5.3. These results are in very good agreement with our primary assumption for linearity of the system model.

Table 5.1. Illuminance read by ambient light sensors during the first experiment in system identification stage. LED2 was kept off during the test.

LED1 dimming levels (percentage)	ALS1 values (Lux)	ALS2 values (Lux)
0	0	0
10	64	40
20	120	80
30	176	120
40	256	176
50	328	224
60	424	289
70	520	356
80	612	424
90	715	496
100	836	588

We could further use different linear regression methods in order to obtain the mathematical model of the system. Among the regression methods, the ordinary least square (OLS) is the simplest but one of the most effective estimators [48]. OLS estimates are commonly used in analyzing both experimental and observational data. This method tries to fit a straight line through the set of n points in such a way that makes the sum of squared residuals of the model (i.e., the vertical distances between the points of the data set and the fitted line) as small as possible.

Table 5.2. Illuminance read by ambient light sensors during the second experiment in system identification stage. LED1 was kept off during the test.

LED2 dimming levels (percentage)	ALS1 values (Lux)	ALS2 values (Lux)
0	0	0
10	48	64
20	72	106
30	112	160
40	144	208
50	183	256
60	233	336
70	288	413
80	344	488
90	401	567
100	473	666

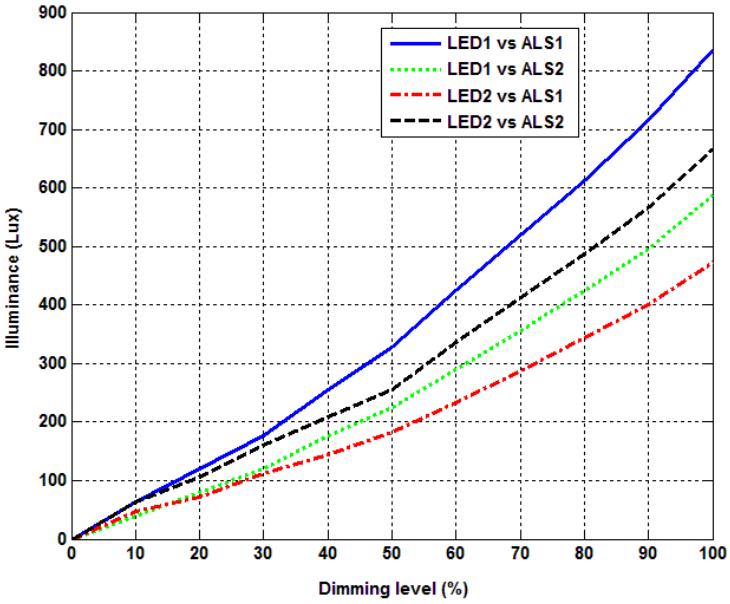

Figure 5.3. Illuminance obtained during the system identification stage.

By adopting the least square method described above, the best fits for our data sets are given as:

$$\begin{aligned} y_{11} &= 8.28x_1 - 46.09, \\ y_{12} &= 5.80x_1 - 36.14, \\ y_{21} &= 4.57x_2 - 10.09, \\ y_{22} &= 6.47x_2 - 27.00, \end{aligned}$$

where y_{ij} in Lux represents the effect of $i-th$ luminaire on the $j-th$ sensor, and x_i is the dimming level of the $i-th$ luminaire. The best fit for each data set is shown in Figure 5.4. All the obtained coefficients are within a 95% confidence bound.

The illuminance at any level is the summation of the lights from all the luminaires in the environment [15]. Thus we would have

$$\begin{aligned} y_1 &= y_{11} + y_{21} = 8.28x_1 + 4.57x_2 - 56.18, \\ y_2 &= y_{12} + y_{22} = 5.80x_1 + 6.47x_2 - 63.14 \Rightarrow \end{aligned}$$

$$\begin{bmatrix} y_1 \\ y_2 \end{bmatrix} = \begin{bmatrix} t_{11} & t_{12} \\ t_{21} & t_{22} \end{bmatrix} \begin{bmatrix} x_1 \\ x_2 \end{bmatrix} + \begin{bmatrix} c_1 \\ c_2 \end{bmatrix} = \begin{bmatrix} 8.28 & 4.57 \\ 5.80 & 6.47 \end{bmatrix} \begin{bmatrix} x_1 \\ x_2 \end{bmatrix} + \begin{bmatrix} -56.18 \\ -63.14 \end{bmatrix}.$$

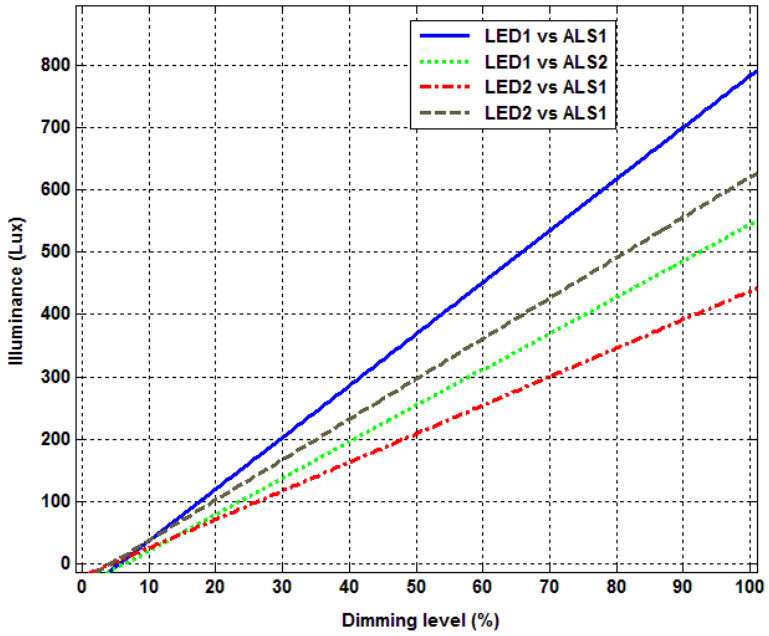

Figure 5.4. Best fits for the data sets obtained during the system identification stage using the ordinary least square method.

Thus the matrix T which represents the model of the system would be:

$$T = \begin{bmatrix} 8.28 & 4.57 \\ 5.80 & 6.47 \end{bmatrix}. \qquad (5.1)$$

The offset matrix C represents the system model uncertainties. This offset could also be interpreted as a constant disturbance (Y_l) in the system model presented in Figure 3.1. It is also proven (i.e., in Chapter 3) that the closed-loop control system is capable of handling the constant disturbances.

5.2. Experimental Results for the Proposed Lighting Control Algorithm

After identifying the system model, various simulations and experiments were carried out to evaluate the effectiveness of the proposed lighting control algorithm. Recalling from Chapter 3, the optimum value for state feedback coefficient K is given by

$$K = \sqrt{\frac{q}{r}} T^T (TT^T)^{-1/2}, \tag{5.2}$$

where q, and r determine the weight of each term in the cost function. By assuming equal weights for both terms (i.e., $q = 0.5$ and $r = 0.5$), the optimum value of matrix K for the system described by (5.1) is

$$K = \sqrt{\frac{0.5}{0.5}} T^T (TT^T)^{-1/2} = \begin{bmatrix} 0.9965 & 0.0831 \\ -0.0831 & 0.9965 \end{bmatrix}.$$

We can also verify the stability of the system by assessing the negative-definiteness of the matrix $(-TK)$. Let assume:

$$Z = -TK = -\begin{bmatrix} 8.28 & 4.57 \\ 5.80 & 6.47 \end{bmatrix} \times \begin{bmatrix} 0.9965 & 0.0831 \\ -0.0831 & 0.9965 \end{bmatrix} = \begin{bmatrix} -7.8716 & -5.2423 \\ -5.2423 & -6.9296 \end{bmatrix}.$$

As matrix Z is a symmetric matrix, it would be negative-definite if and only if all of its eigenvalues are negative [49]. By calculating the eigenvalues of matrix Z, we would have $\lambda_1 = -12.66$ and $\lambda_2 = -2.13$, which confirms the asymptotic stability of the system. This also confirms the convergence of error to zero in the proposed closed-loop system.

After finding the optimum value of matrix K, the first set of experiments were carried out to confirm the main objective of the system, i.e., delivering the target illuminance at each sensor. To this end a series of different desired values were fed to the system as the reference inputs and the response of the system to each of them were recorded and further used for the analysis.

The first series of experiments were carried out by setting the both desired light levels to 600Lux. Figure 5.5 shows the error of the closed-loop control system for the first 50 seconds with both r, and q set to 0.5, simulated by Matlab/Simulink. Instead of demonstrating the percentage or the absolute value of the error, the exact difference between the desired value and the output value at each time step is reported. Positive error values can be interpreted as the lack of satisfactory light, while negative values represents the over illumination state. The results confirm the convergence of the error to zero in the closed-loop control system. Depicted in Figure 5.6 are the dimming levels trajectory for each luminaire during the simulation period. Recalling from Chapter 3, it has been proven that the proposed cost function would have a minimum value when the optimum K is used as the state feedback in the system. This fact was also investigated during the experiments. Figure 5.7 shows the variation of the cost function for different K values near its optimum value. This figure illustrates the final value of the cost function of various systems with arbitrary state feedback matrix $\acute{K}$, where $\acute{K} = K - \delta$. As it was anticipated, when $\delta = 0$ (i.e., system with optimum state feedback K), the minimum value of cost function will be achieved.

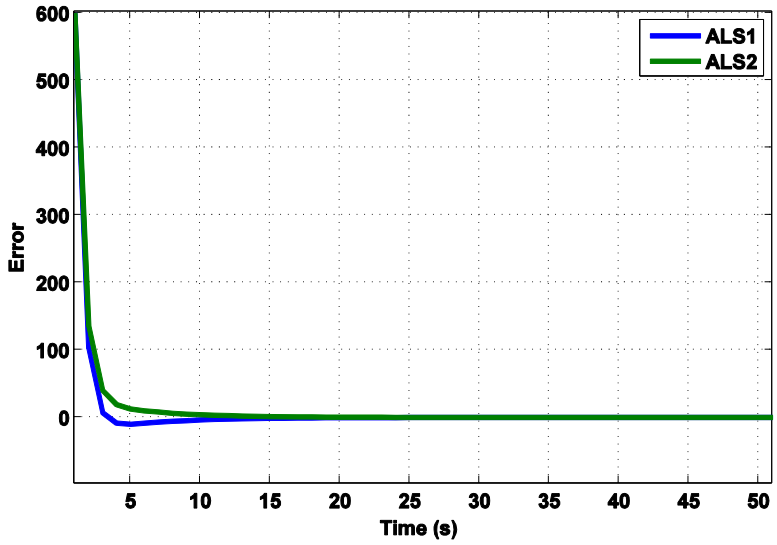

Figure 5.5. Error of the closed-loop system obtained by the simulation. Both target illuminance were set to 600Lux and $r = q = 0.5$.

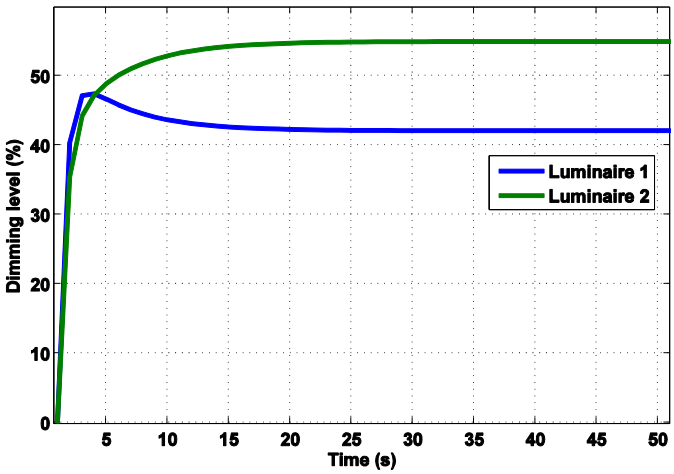

Figure 5.6. Trajectories of the inputs (i.e., dimming levels) in the closed-loop system, obtained by the simulation. Both target illuminance were set to 600Lux and $r = q = 0.5$.

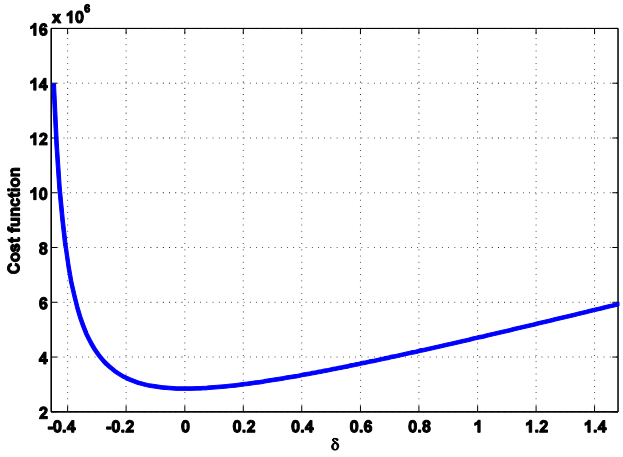

Figure 5.7. Variation of the cost function for different K near its optimum value (i.e., $\delta = 0$). Both target illuminance were set to 600Lux and $r = q = 0.5$.

The above test was also carried out in a real environment using the implemented test bed. Figure 5.8 shows the error of the closed-loop control system in the first 50 seconds, where both r, and q are equal to 0.5. It can be seen that the obtained results are in very good agreement with the simulation results. This fact further confirms that the obtained model is very close to the real model of the system. The results also verified the convergence of the error to zero. Depicted in Figure 5.9 are the dimming level trajectories for each luminaire during this experiment.

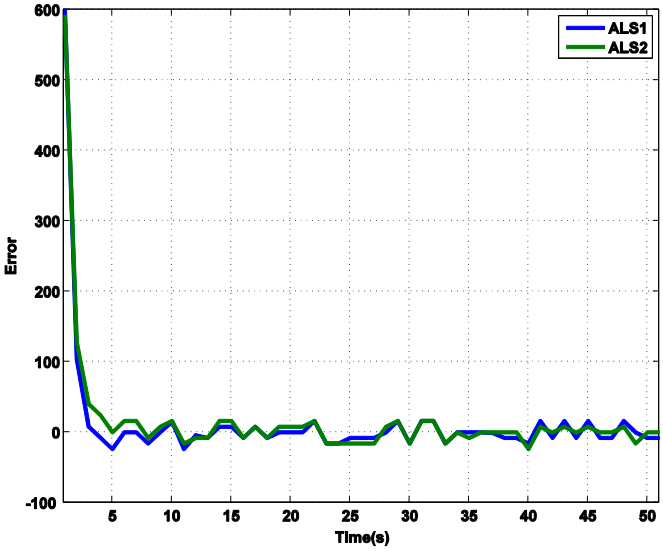

Figure 5.8. Error of the closed-loop system obtained from real experiment. Both target illuminance were set to 600Lux and $r = q = 0.5$.

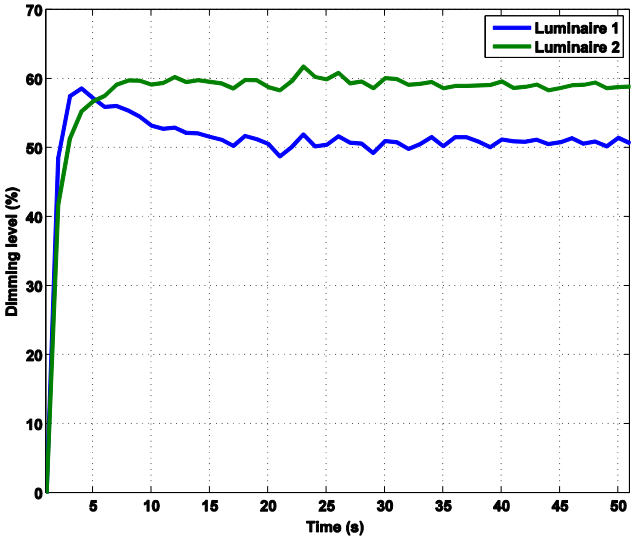

Figure 5.9. Trajectories of the inputs (i.e., dimming levels) in the closed-loop system, obtained from real experiment. Both target illuminance were set to 600Lux and $r = q = 0.5$.

Two more experiments were carried out for different sets of r and q. In the first experiment, q and r were set to 0.1 and 0.9, respectively. Figure 5.10 shows the error of the system in 50 seconds, where $r = 0.9$ and $q = 0.1$. The dimming level trajectories of the luminaires are illustrated in Figure 5.11 as well. Figures 5.13 and 5.14 show the error

and system input values for the same experiment carried out in the real environment. The obtained results from both simulation and the experiments demonstrate that by adopting the new values for r and q, the error speed of convergence is sacrificed at the cost of smoother transition in the inputs of the system.

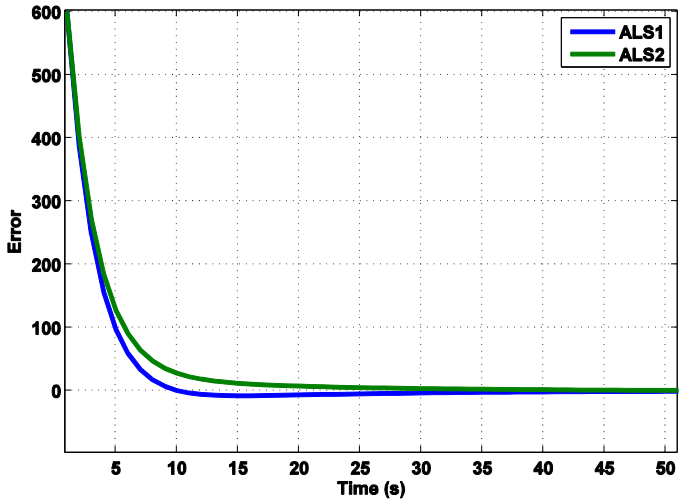

Figure 5.10. Error of the closed-loop system obtained by the simulation. Both target illuminance were set to 600Lux ($r = 0.9$ and $q = 0.1$).

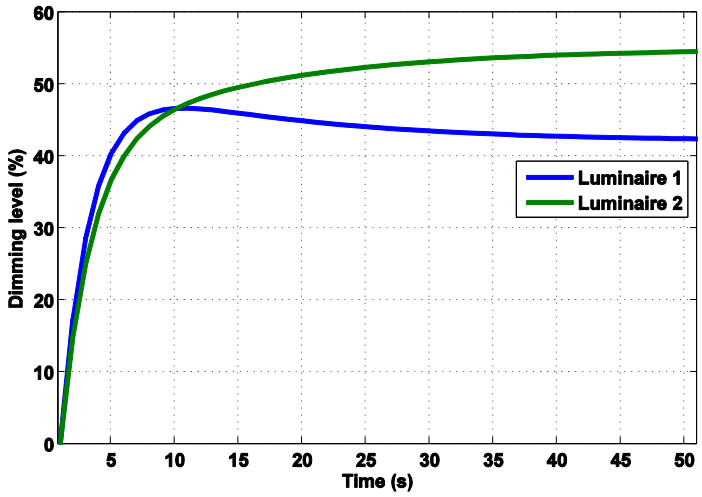

Figure 5.11. Trajectories of the inputs (i.e., dimming levels) in the closed-loop system, obtained by simulation. Both target illuminance were set to 600Lux ($r = 0.9$ and $q = 0.1$).

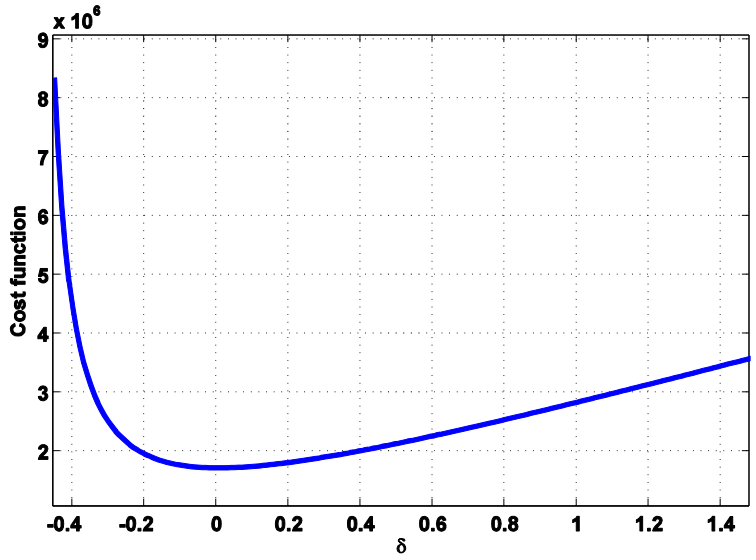

Figure 5.12. Variation of the cost function for different K near its optimum value (i.e., $\delta = 0$). Both target illuminance were set to 600Lux ($r = 0.9$ and $q = 0.1$).

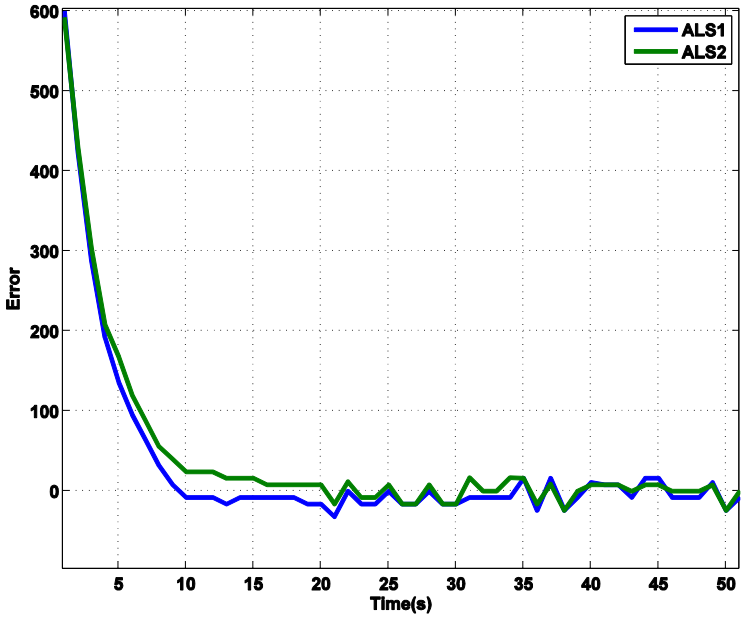

Figure 5.13. Error of the closed-loop system obtained from real experiments. Both target illuminance were set to 600Lux ($r = 0.9$ and $q = 0.1$).

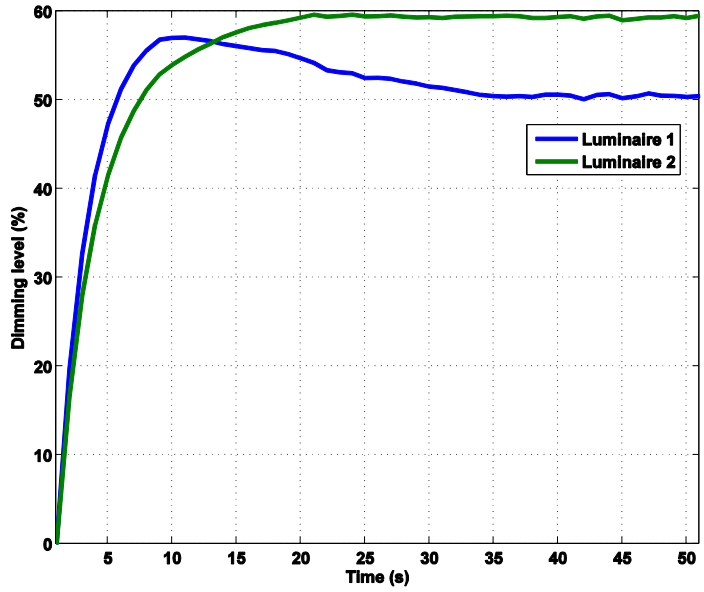

Figure 5.14. Trajectories of the inputs (i.e., dimming levels) in the closed-loop system, obtained from real experiments simulation. Both target illuminance were set to 600Lux ($r = 0.9$ and $q = 0.1$).

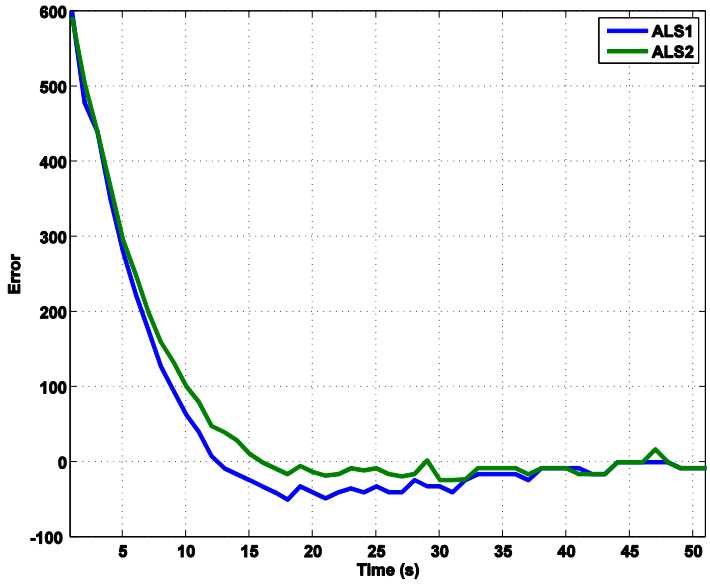

Figure 5.15. Error of the closed-loop system obtained from real experiments. Both target illuminance were set to 600Lux, $r = 0.95$ and $q = 0.05$.

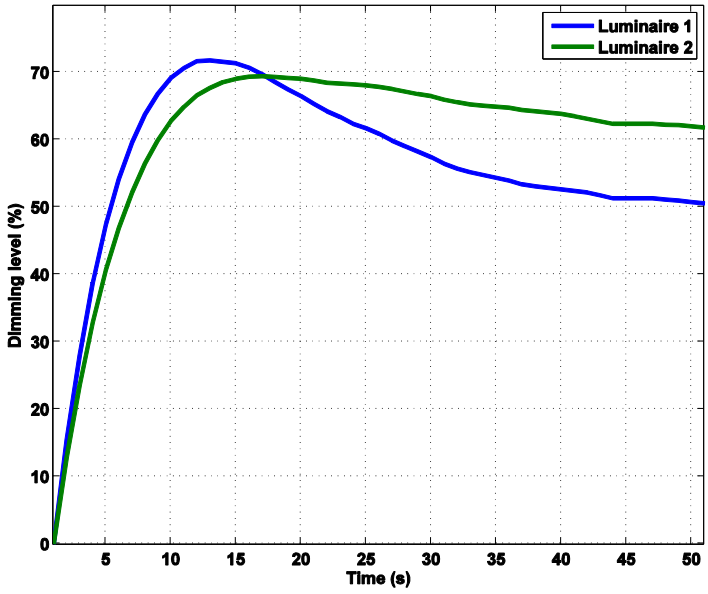

Figure 5.16. Trajectories of the inputs (i.e., dimming levels) in the closed-loop system, obtained from real experiments. Both target illuminance were set to 600Lux, $r = 0.95$ and $q = 0.05$.

Similar experiments were carried out in the real environment by choosing other values for r and q, i.e., $r = 0.05$ and $q = 0.95$. Figures 5.15 and 5.16 illustrate the error of the closed-loop control system and input values obtained in this experiment, respectively.

Similar experiments were carried out by varying set point values. In this test the desired value for the ALS1 was set to 500Lux, while 400Lux was selected for ALS2. The weights q and r were also set to 0.1 and 0.9, respectively. Figure 5.17, 5.18 and 5.19 show the results obtained from simulation and Figure 5.20 and 5.21 illustrate the results obtained by experiments. As can be seen from these figures, the experimental results are in very good agreement with simulation results.

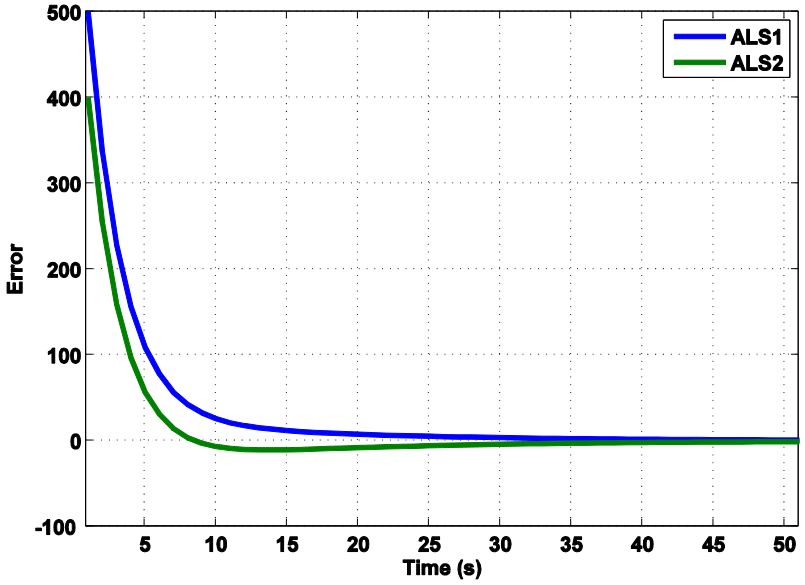

Figure 5.17. Error of the closed-loop system obtained by the simulation ($r = 0.9$ and $q = 0.1$). Target illuminance for ALS1 was set to 500Lux, while 400Lux was the selected target for ALS2.

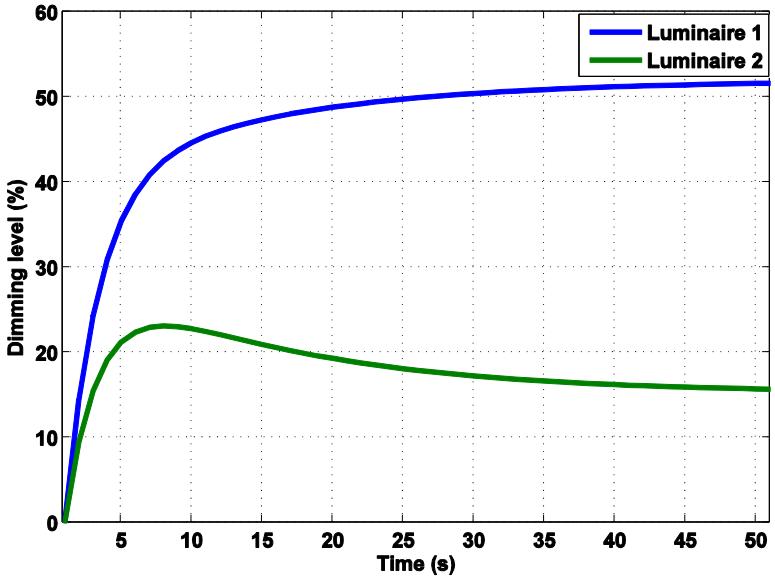

Figure 5.18. Trajectories of the inputs (i.e., dimming levels) in the closed-loop system obtained by the simulation ($r = 0.9$ and $q = 0.1$). Target illuminance for ALS1 was set to 500Lux, while 400Lux was the selected target for ALS2.

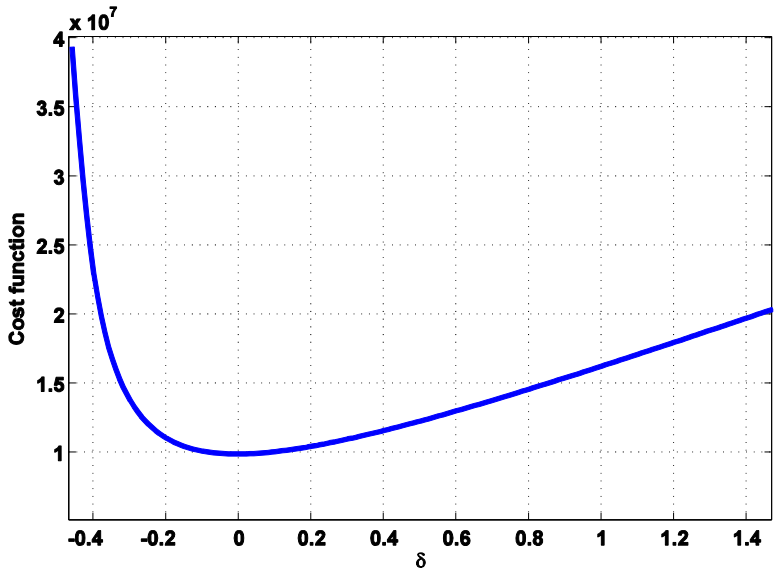

Figure 5.19. Variation of the cost function for different K near its optimum value (i.e., $\delta = 0$). Target illuminance for ALS1 was set to 500Lux, while 400Lux was the selected target for ALS2 ($r = 0.9$ and $q = 0.1$).

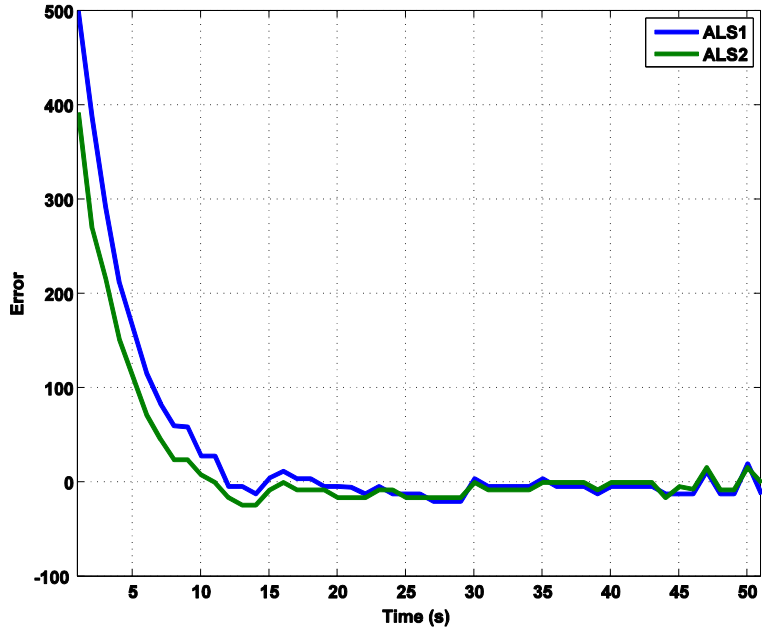

Figure 5.20. Error of the closed-loop system obtained from the real experiment ($r = 0.9$ and $q = 0.1$). Target illuminance for ALS1 was set to 500Lux, while 400Lux was the selected target for ALS2.

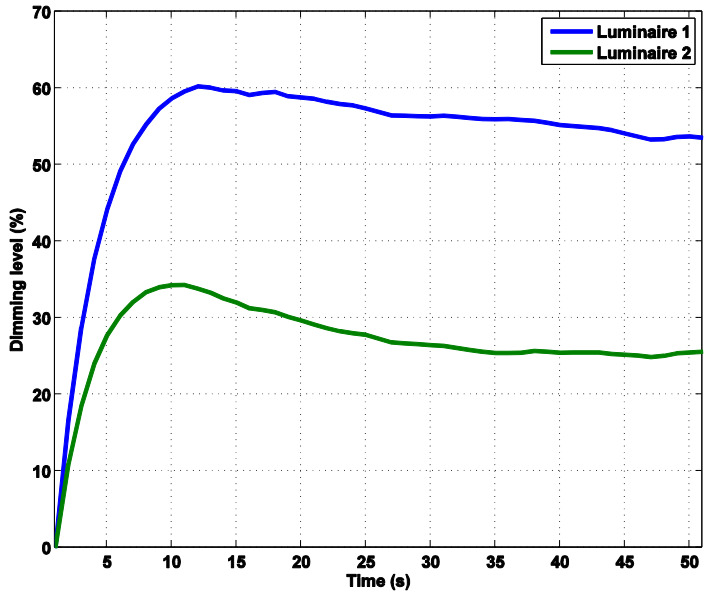

Figure 5.21. Trajectories of the inputs (i.e., dimming levels) in the closed-loop system obtained from the real experiment ($r = 0.9$ and $q = 0.1$). Target illuminance for ALS1 was set to 500Lux, while 400Lux was the selected target for ALS2.

To verify stability of the proposed control system, three more test scenarios were carried out. The first scenario studied system behavior when it is fed by a pair of non-achievable reference inputs. For instance, 500Lux and 250Lux outputs in the experimental setup would not be achievable. This fact could be easily verified by assessing the illuminance values obtained during the system identification shown in Table 5.1. The reported values clearly show that whenever the illuminance of the ALS1 reaches to 500Lux, there would be at least 350Lux reading on the ALS2, thus making the pair of 500Lux and 250Lux physically impossible to reach. This fact also implies that there would be no need for the second luminaire to be working at all, hence reducing the amount of energy consumption by the system. Thus the proposed control algorithm can reduce the amount of energy consumption. The results from this experiment confirm the above argument. Figures 5.22 and 5.23 illustrate the error and the inputs of the closed-loop system in the experiment. As demonstrated in Figure 5.23, the dimming level of the second luminaire converges to zero in which shows the attempt by the control algorithm to minimize the error. This also confirms that the proposed method could reduce the amount of energy consumption when there are potential overlaps between the desired light levels selected by the users.

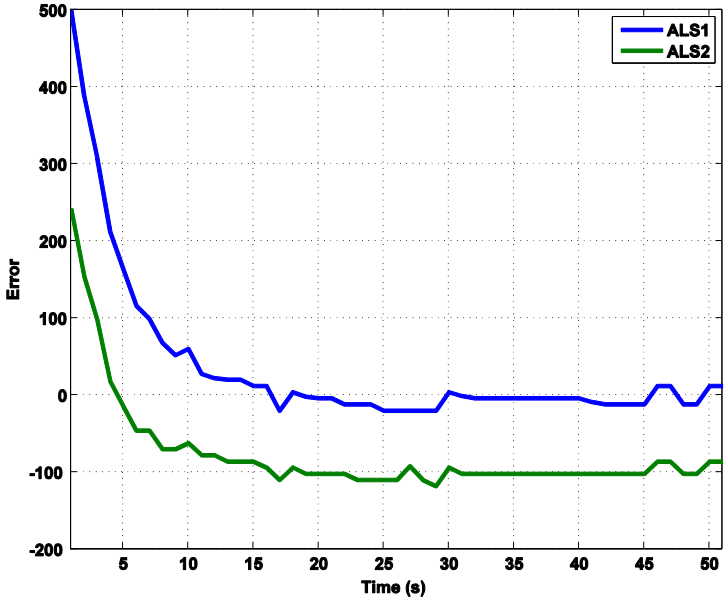

Figure 5.22. Error of the closed-loop system obtained from real experiment ($r = 0.9$ and $q = 0.1$). Target illuminance is set to a non-achievable pair of 500Lux and 250Lux for ALS1 and ALS2 respectively.

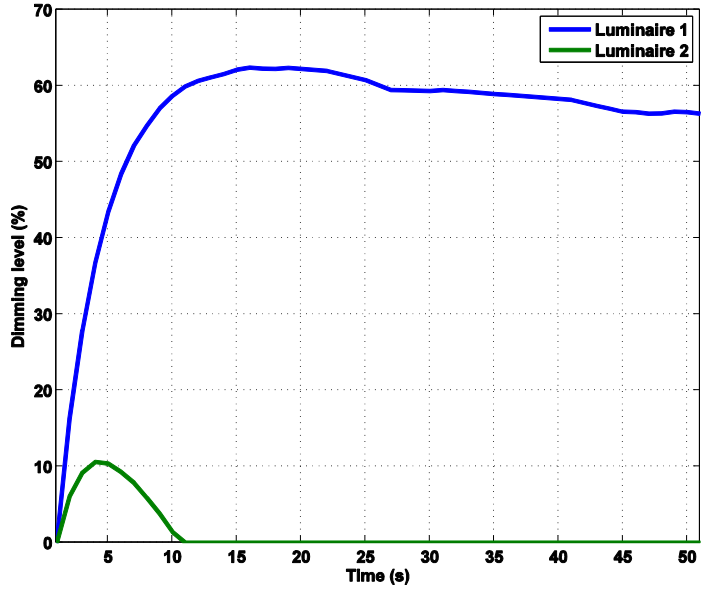

Figure 5.23. Trajectories of the inputs (i.e., dimming levels) in the closed-loop system obtained from real experiment ($r = 0.9$ and $q = 0.1$). Target illuminance is set to a non-achievable pair of 500Lux and 250Lux for ALS1 and ALS2 respectively.

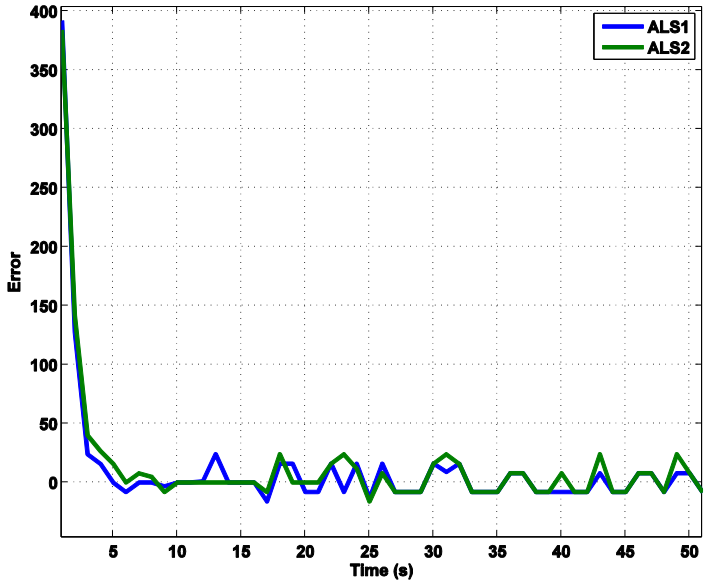

Figure 5.24. Error of the closed-loop system obtained from the real experiment with constant disturbance of 200Lux ($r = q = 0.5$). Both target illuminance were set to 600Lux.

The second scenario targeted the daylight harvesting aspect of the system. Recalling from Chapter 3, the daylight was considered as a constant disturbance to the system. Most of the time, the daylight disturbance could be treated as a good disturbance where it helps the system by compensating a portion or the whole share of the desired illuminance. The effect of daylight on the error and inputs of the proposed control system is demonstrated in Figure 5.24 and Figure 5.25. In this experiment, the desired light levels were both set to 600lux while a constant disturbance of 200lux was applied to the system for the entire test process. By comparing the final values achieved at the end of this experiment with the values achieved by the end of an experiment with no daylight involvement (Shown in Figure 5.19), it is concluded that at least 20% reduction in the amount of power consumed can be achieved.

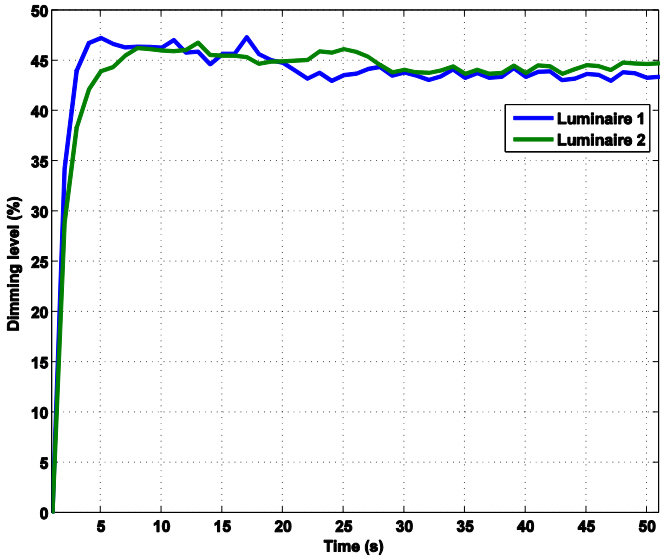

Figure 5.25. Trajectories of the inputs (i.e., dimming levels) in the closed-loop system obtained from the real experiment ($r = q = 0.5$). Both target illuminance were set to 600Lux (constant disturbance of 200Lux was imposed to the system).

The third experiment was carried out to test the behavior of the system when an unexpected large disturbance was applied. The procedure was very similar to the previous experiment where both the desired illuminance were set to 600lux. For two short periods during the test, with the help of artificial lights, both sensors where exposed to a sudden large amount of light. The light was turned off afterward. The error plots are shown in Figure 5.26. The maximum illuminance that the light sensors were able to measure were 1000 Lux for both sensors. This behavior justifies the error of -400 (i.e., $e = y_d - y = 600 - 1000 = -400$Lux) shown in this figure. Considering the trajectory of the dimming levels shown in figure 5.27, it follows that whenever the system was exposed to a large amount of outside light, it tried to minimize the error by reducing the amount of light produced by its own luminaires, eventually turning them off. Furthermore, by removing the imposed disturbance, the system was fast enough to sense sudden removal of the disturbance and turning the lights on again to provide satisfactory light levels.

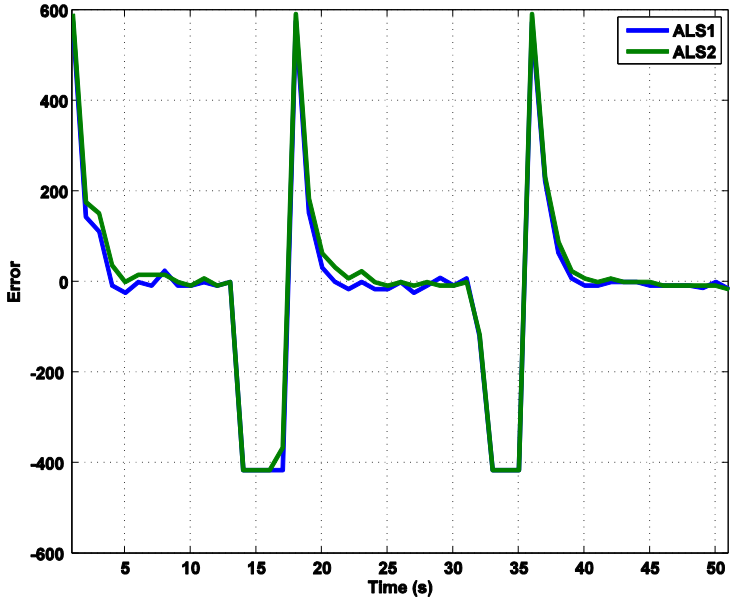

Figure 5.26. Error of the closed-loop system obtained from real experiment ($r = q = 0.5$). System were twice exposed to a large amount of light disturbance. Both target illuminance were set to 600Lux.

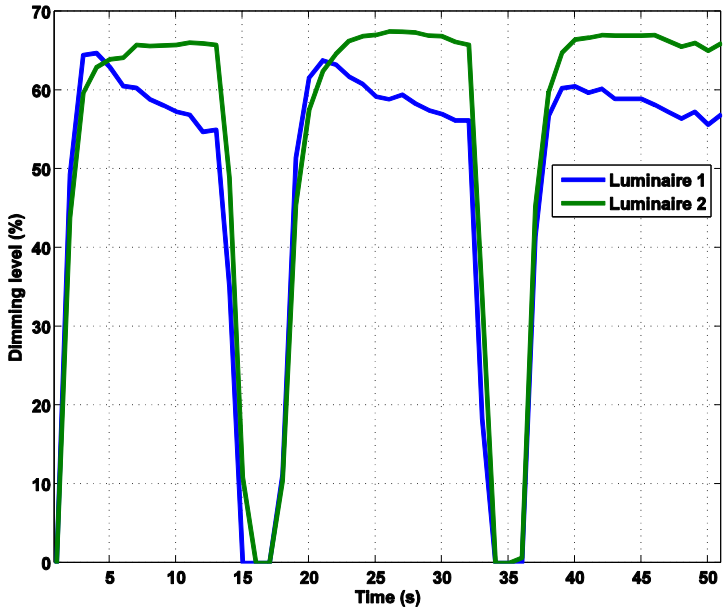

Figure 5.27. Trajectories of the inputs (i.e., dimming levels) in the closed-loop system obtained from the real experiment ($r = q = 0.5$). System were twice exposed to a large amount of light disturbance. Both target illuminance were set to 600Lux.

The last experiment was mostly concerned with the performance of the proposed algorithm in a non-square system model (i.e., the number of luminaires and the light sensors are not equal). To better demonstrate the behavior of the proposed method, a simple non-square full rank matrix T given by

$$T = \begin{bmatrix} 1 & 1 & 1 \\ 1 & 1 & 2 \end{bmatrix}$$

was chosen as our hypothetical lighting system model. Recalling from Chapter 3, when the number of inputs is larger than the number of outputs, we have an over-actuated system which can generally have multiple solutions. Figure 5.28 illustrate the error of the closed-loop control system with the desired lux levels set to 3Lux and 5Lux. The optimum K obtained from (5.2) was also used as the linear time-invariant state feedback. Note that the matrix T in (5.2) is replaced with the 2×2 matrix B, where:

$$B = \begin{bmatrix} -0.56 & -0.82 \\ -0.82 & 0.56 \end{bmatrix},$$

is orthonormal basis vector of the matrix T. Figure 5.29 illustrates the trajectories of the inputs in the closed-loop control system for the optimum K. One interesting observation could be the final

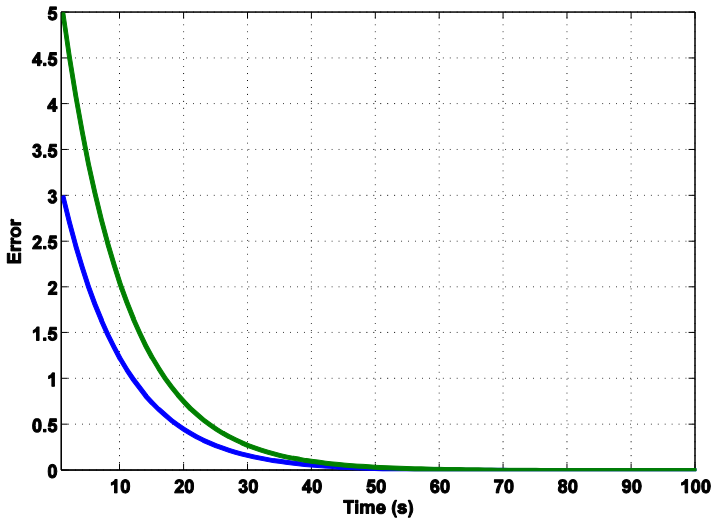

Figure 5.28. Error of the closed-loop system with a non-square matrix plant model. The target illuminance were set to 3 and 5 Lux respectively.

values of the inputs achieved by the proposed control algorithm. The combination of input values $u_1 = 0.5, u_2 = 0.5\ and\ u_3 = 2$ would make the sum of the square of the inputs (i.e., $u_1^2 + u_2^2 + u_3^2$) minimum, hence satisfying the objective of minimizing the input power.

Figure 5.30 also illustrates the input trajectories of the closed-loop control system for the same set point, but with different values for the state feedback K. In both cases, the error of the closed-loop feedback would converge to zero.

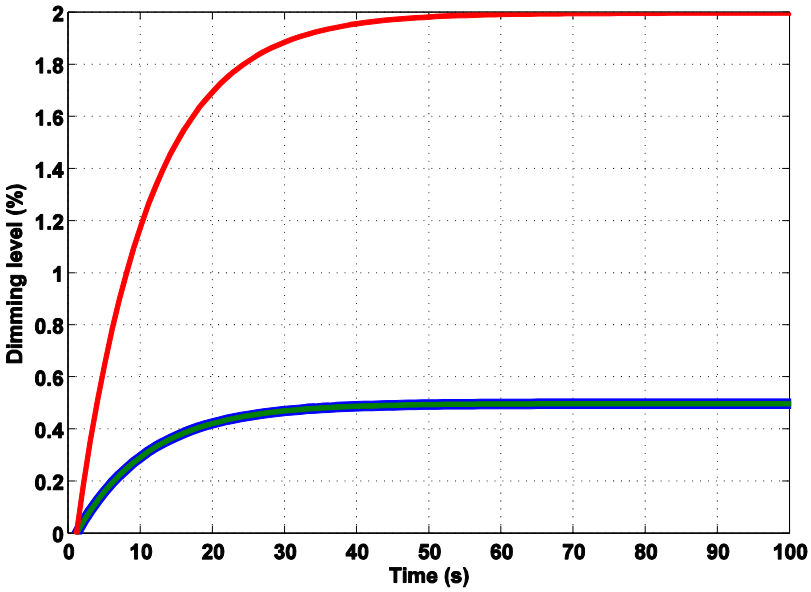

Figure 5.29. Trajectories of the inputs (i.e., dimming levels) in the closed-loop system with a non-square matrix plant model. The target illuminance were set to 3 and 5 Lux respectively. Note that the first and second inputs follow a very similar trajectory. The optimum value for matrix K was used in this experiment.

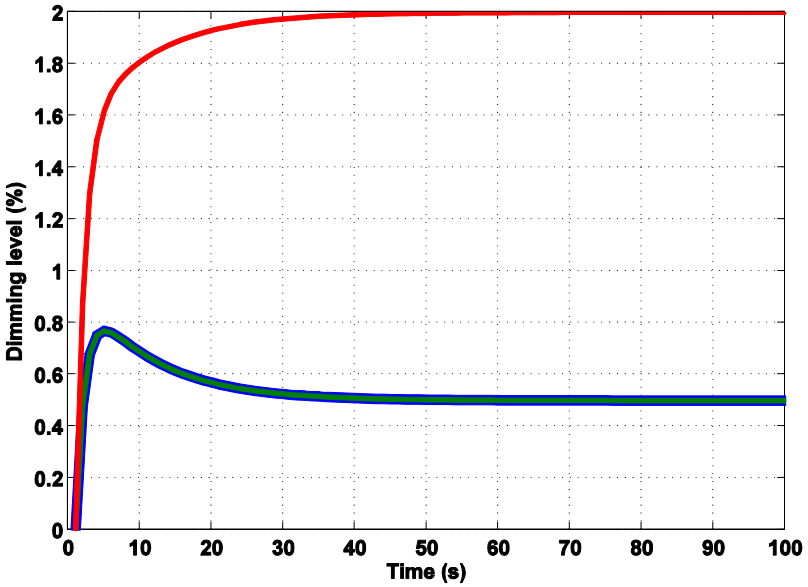

a

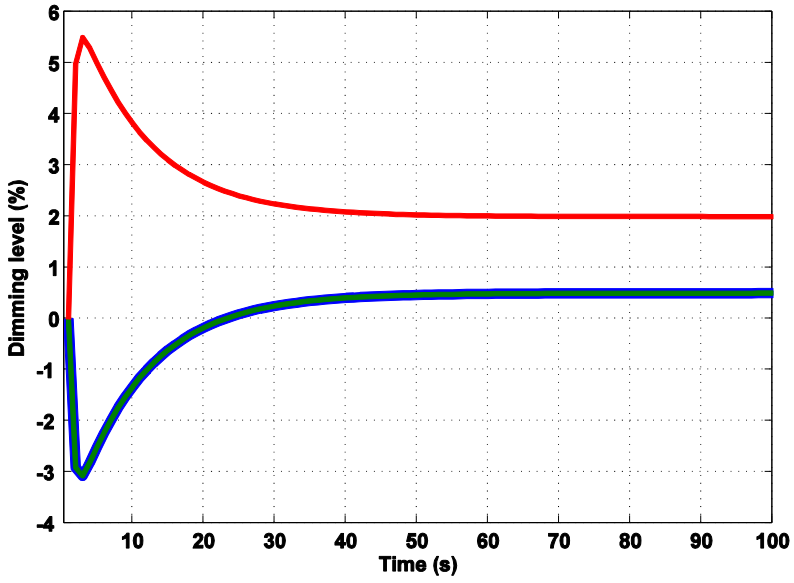

b

Figure 5.30. (a) and (b): Effects of using non-optimum state feedback K on the trajectories of the inputs (i.e., dimming levels) in the closed-loop system with a non-square matrix plant model. The target illuminance were set to 3 and 5 Lux respectively. Note that the first and second inputs follow a very similar trajectory.

Chapter 6. Conclusions and Future Works

This thesis has two main contributions. First, a robust communication framework was developed as a main pre-requisite for deployment of any lighting system. The developed framework is responsible for facilitating the communication between various type of hardware such as occupancy, motion, and light sensors, as well as light actuators in the network. Daylight harvesting, occupancy detection, and light level tuning were different strategies adopted by the developed lighting system. Second, we have proposed a lighting control algorithm which has the potential to satisfy the visual preferences of the users while reducing the overall amount of energy usage in the system. The proposed algorithm is capable of delivering the desired light levels for each occupant. The effectiveness of the developed intelligent lighting framework and the proposed control algorithm were verified in two separate pilot implementations. The most important conclusion that could be drawn is that promising amounts of energy savings can be obtained by implementing the proposed lighting system. Also the proposed lighting control algorithm was proven to be successful in delivering the desired light levels at specific points. The obtained results from both pilot implementations shows that further incorporation of the proposed lighting control algorithm in the developed lighting framework for large scale implementations in the buildings could be very promising in terms of both satisfying the users' visual preferences and minimizing the amount of power consumption in the buildings. Thus the future work would include integration of the proposed control algorithm in an actual lighting system in a building environment. This could be a very challenging work indeed where the coordination of data, data transmission rates, and network delays could degrade performance of the proposed lighting control algorithm.

Another potential work could be incorporating the input vector constraints with the LQR controller. The conventional LQR controller does not put any restriction on the input signals. Thus the amplitude of the optimized input vector may turn out to be well above the physical constraints of the controller, causing the system to be saturated. Hence designing a LQR controller which can compensate for the violation of the input constraints could be an interesting subject for the future studies in this field.

Another direction of study could be investigating the possible uses of the extra inputs in over-actuated lighting systems. Minimum-norm solution of input vector obtained from (3.28) will minimize the power consumption of the lighting system, but not necessarily improves the other performance criteria such as light distribution uniformity. Thus by defining different performance criteria, these extra inputs could be used to satisfy the desired performance aspects.

Another potential work could be including learning strategies in the developed lighting framework to help the system learn about the users' preferences and gradually adapt to the users routines; hence improving the performance of the system over the time.

Reference

[1] "International Energy Agency" [Online]. Available: www.iea.org. [Accessed 10 2013].

[2] "Organisation for Economic Co-operation and Development" [Online]. Available: http://www.oecd.org/. [Accessed 10 2013].

[3] "U.S. Energy Information Administration" [Online]. Available: www.eia.org. [Accessed 10 2013].

[4] M. Miki, T. Hiroyasu and K. Imazato, "Proposal for an intelligent lighting system, and verification of control method effectiveness" in *IEEE conference on cybernetics and intelligent systems*, Singapore, 2004.

[5] Y.J. Wen and A. Agogino, "Control of wireles-networked lighting in open-plan offices" *Lighting research and technology,* vol. 43, no. 2, pp. 235-248, 2011.

[6] J. Alonso, "Intelligent control system for fluorescent lighting based on LonWorks technology" in *Conference of industrial electronics society* , Aachen, 1998.

[7] F. Rubinstein and M. Siminovitch, "Fifty percent energy savings with automatic ligthing controls" *IEEE transaction on industry application,* vol. 29, no. 4, pp. 768-773, 1993.

[8] D. Peterson and F. Rubinstein, "Effective lighting control" in *Lighting design and applications*, 1983.

[9] P. Littlefair, "Predicting lighting energy use under daylight linked lighting controls" *Building research and information,* vol. 26, no. 4, pp. 208-222, 1998.

[10] D. H. Li and J. C. Lam, "An investigation of daylighting performance and energy saving in a daylit corridor" *Energy and buildings,* vol. 35, no. 4, pp. 363-373, 2003.

[11] M. Miki and T. Hiroyasu, "Intelligent lighting control using correlation coefficient between luminance and illuminance" in *IASTED Intelligent systems and controls*, 2005.

[12] A. Guillemin, "Using genetic algorithms to take into account user wishes in an advanced buidling control system" Ecole polytechnique federale de lausanne, 2003.

[13] D. Lindelhof, "Bayasian optimization of visual comfort" Ecolo polytechnique federale de lausanne, 2007.

[14] R. Paulson, C. Basu, A. M. Agogino and S. Poll, "Inverse modeling using a wireless sensor network for personalized daylight harvesting", 2013.

[15] Y. Gao, Y. Lin and Y. Sun, "A wireless sensor network based on the novel concept of an I-matrix to achieve high-precision lighting control" *Building and environment,* vol. 70, pp. 223-232, 2013.

[16] H. Kim and T.-G. Kang, "Autonomous lighting control based on adjustable illumination model" in *International conference on information science and applications*, 2013.

[17] A. Albert, Regression and the Moore-Penrose pseudoinverse, Burlington, MA: Elsevier, 1972.

[18] C.H. Huang, C.C. Huang, C.C. Chiang, Z.Y. Yuan, B.R. Shi and Y.T. Su, "Development of smart illumination system with fuzzy logic theory" in *International conference on computer, networks and communication engineering*, 2013.

[19] L. Ciabattoni, A. Freddi, G. Ippoliti, M. Marcantonio, D. Marchei, A. Monteriu and M. Pirro, "A smart lighting system for industrial and domestic use" in *IEEE international conference on mechatronics*, 2013.

[20] S. H. Lee and J. K. Kwon, "Distributed dimming control for LED" *Optics express,* vol. 21, no. S6, pp. 917-932, 2013.

[21] "IEEE 802 LAN/MAN standards committee" [Online]. Available: http://www.ieee802.org/. [Accessed 10 2013].

[22] J. Day and H. Zimmermann, "The OSI reference model" in *Proceeding of IEEE*, 1983.

[23] J. F. Kurose and K. Ross, Computer networking: A Top-Down approach 4/E, Addison-Wesley, 2007.

[24] B. A. Forouzan and S. Chung Fegan, Data communications and networking, McGraw-Hill Higher Education, 2003.

[25] "Wi-Fi Alliance" [Online]. Available: http://www.wi-fi.org/. [Accessed 10 2013].

[26] J. M. Tjensvold, "Comparison of the IEEE 802.11, 802.15.1, 802.15.4 and 802.15.6 wireless standards", 2007.

[27] "ZigBee Alliance" [Online]. Available: http://www.zigbee.org/. [Accessed 10 2013].

[28] M. Petrova, J. Riihijarvi, P. Mahonen and S. Labella, "Performance study of IEEE 802.15.4 using measurements and simulations" in *IEEE wireless communications and networking conference*, 2006.

[29] "Bluetooth SIG" [Online]. Available: http://www.bluetooth.com. [Accessed 10 2013].

[30] N. Golmie, N. Chevrollier and O. Rebala, "Bluetooth and WLAN coexistence: challenges and solutions," in *IEEE wireless communications*, 2003.

[31] E. Georgakakis, S. A. Nikolidakis, D. D. Vergados and C. Douligeris, "An analysis of Bluetooth, Zigbee and Bluetooth Low Energy and their use in WBANs" *Wireless Mobile Communication and Healthcare,* vol. 55, pp. 168-175, 2011.

[32] "NXP low power RF" [Online]. Available: http://www.jennic.com/. [Accessed 10 2013].

[33] H.-J. Chiu, Y.-K. Lo, J.-T. Chen, S.-J. Cheng, C.-Y. Lin and S.-C. Mou, "A High-Efficiency dimmable LED driver for low-power lighting applications" *IEEE transactions on industrial electronics,* vol. 57, no. 2, pp. 735-743, 2010.

[34] S. Hui and Y. Qin, "A general photo-electro-thermal theory for Light Emitting Diode (LED) systems" *IEEE transactions on power electronics,* vol. 24, no. 8, pp. 1967-1976, 2009.

[35] E. M. Gutsait, "Analysis of LED modules for local illumination" *Journal of coomunication technology and electronics,* vol. 52, no. 12, pp. 1377-1395, 2009.

[36] A. Ryer, "Light measurement handbook" Int. Lights Inc, 1998.

[37] A. V. Oppenheim, A. S. Willsky and S. H. Nawab, Signals and systems, Prentice Hall, 1997.

[38] F. W. Fairman, Linear control theory, the state space approach, Chichester, New York: Wiley, 1998.

[39] P. Albertos and A. Sala, Multivariable control systems, pringer, 2004.

[40] K. Zhou and J. Doyle, Essential of robust control, NJ: Prentice Hall, Engle-wood Cliffs, 1998.

[41] "LQI Notes" [Online]. Available: http://www.egr.msu.edu/classes/me851/jchoi/lecture/LQI-note.pdf. [Accessed 10 2013].

[42] "Cree Inc." [Online]. Available: http://www.cree.com/Lighting/Products/Indoor/Troffers-International/CR22-220V-240V. [Accessed 10 2013].

[43] P. R. Boyce, J. A. Veitch, G. R. Newsham, C. C. Jones, J. Heerwagen, M. Myer and C. M. Hunter, "Occupant use of switching and dimming controls in offices" *Lighting research and technology,* vol. 38, pp. 358-376, 2006.

[44] C. DiLouie, "Personal lighting control can increase worker satisfaction and motivation" Buildings.com, 2004.

[45] "Xeleum Corporation" [Online]. Available: http://www.xeleum.com/announcements/accessories-for-xeleum-troffers. [Accessed 10 2013].

[46] "BDS Industrial Solution Inc." [Online]. Available: http://www.bdsindustrial.com/catalogue/index.php?categoryID=154. [Accessed 10 2013].

[47] "Texas Instruments" [Online]. Available: http://www.ti.com/lsds/ti/microcontroller/16-bit_msp430/overview.page. [Accessed 10 2013].

[48] N. H. Bingham and J. M. Fry, Regression: linear models in statistics, Springer, 2010.

[49] R. A. Horn and C. R. Johnson, Matrix analysis, Cambridge University Press, 1990.

[50] "Lighting controls" in *International light revision*, 1998.